ESTIMATION OF SPACECRAFT ATTITUDE IN THE PRESENCE OF UNMODELED DISTURBANCE TORQUES

by

Earl Douglas Pinson

Thesis submitted to the faculty of the

Virginia Polytechnic Institute and State University

in partial fulfillment of the requirements for

the degree of

MASTER OF SCIENCE

in

Engineering Mechanics

APPROVED:

J. L. Junkins

R. A. Heller

L. G. Kraige

August, 1984

Blacksburg, Virginia

ACKNOWLEDGEMENTS

I wish to acknowledge the guidance and friendship of Dr. John L. Junkins throughout the course of this research. The hours spent in the classroom and his office have proven to be most beneficial and are greatly appreciated.

Thanks is also due to Mr. D. J. Mook for programming support and consultation, to Mr. Joseph Miner for assistance in the preparation of various visual aids contained in this thesis, and to Mrs. Vanessa Mc Coy for her assistance in copying, reducing and modifying the figures in Chapter 5. I am most grateful to these people for sharing their knowledge, experience and expertise.

The moral support, occasional prod and typing skills of my wife, Marcella C. Pinson, are also deserving of special thanks.

TABLE OF CONTENTS

LIST OF FIGURES

LIST OF TABLES

CHAPTER 1

INTRODUCTION

Since the first satellite was launched, finding sufficiently precise orientation estimates at any time after launch has been a difficult task. The first inertial reference system (IRS) yielded errors in attitude that, in some cases, would be intolerable now, but over the years of analytical and hardware advances, these errors have been trimmed dramatically.

The translational position of an orbiting object may be determined by radar tracking, but the orientation cannot be measured adequately except by an on-board system of sensors. (The orientation of a spacecraft may be determined by other means if special signal reflectors are mounted on the craft in various locations.) Reliably estimating the orientation of a satellite is almost always accomplished by some combination of star sensors, sun sensors, horizon sensors, and rate gyroscopes. The orientation determination schemes discussed herein are assumed to employ a slit-type star sensing system to detect the line-of-sight vector to stars at discrete instants, in conjunction with a rate gyroscope system to measure angular velocity.

The first type of on-board IRS to be used historically

is known as a gimballed or stabilized platform system. In this method of attitude determination, a part of the craft (known as a platform) is aligned in inertially fixed directions before the launch and the future attitude of the craft is measured from this inertially-fixed (ideally) platform. The platform is made to stay in the same orientation relative to a pre-determined reference system by storing angular momentum in a system of gyroscopes, whose axes are fixed with respect to the platform, and thereby making the platform resistant to the small (ideally zero) gimbal torques that would ordinarily change its orientation. For many years, the stabilized platform provided the most accurate estimate of the attitude of an orbiting object. This is not to imply that the method is obsolete - it still provides results as accurate as those provided by many other systems. However, the inevitable slow drift of the inertial platform causes an uncertain bias to develop between the platform and the "true" inertial frame. Thus the orientation of the stabilized platform needs to be re-determined from time to time by a navigation fix.

Competing with the stabilized platform is an IRS known as a strapdown navigation system. In this system the orientation of the spacecraft is determined by the measurements from several rate gyroscopes whose axes are

fixed with respect to the spacecraft itself. This method was initially used in the 1950's[1] and has been improved continuously since then[2,3]. There are several types of gyroscopes that could be used in this system - the most accurate of which is the newly investigated laser gyroscope. This type of "gyroscope" is really not a gyroscope in the strict sense of the word - nothing is spinning - but it promises the greatest accuracy in future applications (see Refs. 2 and 4). This thesis deals with the strapdown concept, but it is not necessary to specify the type of angular velocity measurement hardware used.

Considerable recent research has been devoted to fine-tuning the strapdown IRS concepts. Errors have been identified and their relative significance has been determined[5,6]. Also from these investigations, a streamlined IRS design process has been developed[7]. In short, it is widely believed that the strapdown IRS coupled with a star sensing system will become more prevalent than its gimballed counterpart.

This thesis addresses the problem of estimating the attitude of a satellite based on data obtained from the rate gyroscopes and star-sensors composing a strapdown IRS. A solution procedure is presented wherein the rate gyroscope data is smoothed and the stellar data is adjusted

by the method of least squares to provide estimates of the spacecraft attitude and rate gyroscope biases about each of the three body-fixed axes.

It is felt that two references listed at the end of this thesis deserve special mention because of their close relation to ideas to be presented here. The first of these articles deals with estimating a time series using a Fourier Series and truncating high frequency contributions to remove unwanted noise. Both of these ideas are central to the method given in this thesis, but the ultimate objective and means of achieving this objective differ in details from those presented in Ref. 20. The authors of this recent article, S. C. Raisinghani and K. D. Bilimoria, propose improvements to the method they discuss when it is found that the record being analyzed possesses very low frequency contributions. The problems they experienced and reported concerning these low frequency phenomena were not found to be a problem in the research presented as a part of this thesis.

The second of these special articles is Ref. 21. The author of this reference, T. G. Shanahan, presents a method of solving for disturbance torques and certain other values. The method presented in Ref. 21 models the attitude motion using Euler's Equations of a multiple rigid body (spacecraft and reaction wheels), and introduces

various models for bearing friction. This reference does not consider the most general case in which the spacecraft dynamics is poorly understood (e. g., due to an inaccurate model of the departures from rigid body motion). The present approach is believed to be general enough to accommodate these poorly modeled systems but, on the other hand, does not take advantage of the possibility that approximate equations of motion can be written.

This thesis is divided into six major sections: kinematics and dynamics (Chapter 2), rate gyroscope data smoothing (Chapter 3), parameter estimation (Chapter 4), numerical examples and analyses (Chapter 5), conclusions and recommendations (Chapter 6) and the appendix. The appendix contains listings of all programs used in the research presented here.

CHAPTER 2

KINEMATICS AND DYNAMICS

2.0 Overview: Chapter two discusses the method used during the course of this research to ascertain the orientation of an orbiting object describing a circular orbit. In this discussion, three important reference frames are introduced - namely the inertial frame (defined by unit vectors $\underline{n}_i$), the orbiting frame (defined by unit vectors $\underline{o}_i$), and the body-fixed frame (defined by unit vectors $\underline{b}_i$). The fact that all three reference frames are right-handed and orthogonal ascribes certain properties to the transformations between them. These transformations and the properties associated with them are discussed in the kinematics section of the chapter.

In the dynamics section of the chapter, the relationship between the forces and moments applied to the orbiting object and the resulting motion are derived and discussed.

2.1 Kinematics - Motion Parameterization: As a precursor to the discussion of the movement of an orbiting spacecraft, coordinates must be defined to relate the orientation of the object to earth-fixed coordinate directions. In the literature on the subject, there are

several methods for parameterizing the orientation of rotating bodies. The most common solution is the specification of a set of Euler angles - sequential rotations about designated unit vectors in triads derived from a "base" coordinate system[8]. Other parameterizations involve Hamilton's quaternions[9], Cayley-Klein parameters, Euler parameters[10], and the nine direction cosines. More obscure conventions also exist, but most are closely tied to the parameterizations listed above.

In keeping with one of the most common practices, the Euler angle parameterization of angular displacements is used throughout this thesis.

Whenever attempting to describe the absolute orientation of an object, the base system mentioned before will often be considered "inertial" or "Newtonian" in nature. In this discussion, the inertial coordinate system is established at the center of the earth with the $\underline{n}_1$ and $\underline{n}_3$ axes spanning the initial orbital plane of the spacecraft (see Fig. 1). Over one orbit, the orbital plane is inertially constant to a high degree of approximation. Since the attitude motion dealt with here is typically only a fraction of an orbit, negligible error is introduced when the assumption of an inertial orbital plane is made.

Once directions are established by the unit vector triad of the inertial frame, transformations may be

employed to re-point successive vector triads in other arbitrary, orthogonal directions. This is accomplished by specifying the elements of three, 3X3 direction cosine matrices (DCMs). These elements to be specified are the cosines of the angles between the i^{th} and j^{th} unit vectors of the new and old coordinate systems respectively. The basic building blocks of a complete specification of an arbitrary three-dimensional rotation are the elementary DCMs for a single rotation about the 3, 2, and 1 axes. These are denoted in this thesis by $DCM_3(*)$, $DCM_2(*)$, and $DCM_1(*)$ and are defined respectively as follows:

$$\begin{bmatrix} c* & s* & 0 \\ -s* & c* & 0 \\ 0 & 0 & 1 \end{bmatrix}, \begin{bmatrix} c* & 0 & -s* \\ 0 & 1 & 0 \\ s* & 0 & c* \end{bmatrix} \& \begin{bmatrix} 1 & 0 & 0 \\ 0 & c* & s* \\ 0 & -s* & c* \end{bmatrix}$$

where * is the angular displacement, c* is the cosine of *, and s* is the sine of *.

These matrices, and the transformation matrices derived from them by multiplying them together in various combinations, belong to a more general class called orthogonal matrices. Matrices in this class posess the property that their determinant is either +1 or -1. If the determinant is +1, the transformation preserves the right-handed character of the unit vectors. Orthogonal matrices are also characterized by the fact that their transpose is equivalent to their inverse. These properties

are proven and discussed further in Ref. 3.

With some thought, one may determine that there are a limited number of sequences of the above "building-block" matrices that "qualify" as an adequate parameterization of a general three-dimensional rotation. There are, in fact, 12 qualifying sequences - distinguished by the fact that no single-rotation DCM given above appears immediately beside itself in "matrix multiplication style" notation. For example, the 1-2-2, etc. sequences do not qualify, but the 1-2-3 and 3-1-3, etc. sequences do qualify. In this notation, with a 1-2-3 rotation sequence as an example, the base triad is first multiplied by DCM_1, then by DCM_2 and finally DCM_3. The issue of "qualification" makes intuitive sense in that repeating any one of these basic DCMs is equivalent to a single rotation about the designated unit vector, the magnitude of which is the sum of the two rotations. Thus only two degrees of freedom are present instead of three - as required to describe a general angular displacement.

In addition to the above consideration of qualification, one more important observation may be made concerning the Euler angle parameterization scheme: By specifying three 90° rotations about reversed, qualifying sequences, it becomes obvious that the final orientation of a unit vector triad is dependent not only on the magnitude

of the Euler angles but also on the order in which the sequential rotations are performed.

From Fig. 1, note that a single rotation about the $\underline{n}_2$ axis will transform the inertial triad to the orbiting triad. This transformation is described as follows:

$$\begin{Bmatrix} \underline{o}_1 \\ \underline{o}_2 \\ \underline{o}_3 \end{Bmatrix} = \begin{bmatrix} c\gamma & 0 & -s\gamma \\ 0 & 1 & 0 \\ s\gamma & 0 & c\gamma \end{bmatrix} \begin{Bmatrix} \underline{n}_1 \\ \underline{n}_2 \\ \underline{n}_3 \end{Bmatrix} \quad \text{or} \quad [\underline{o}] = DCM_2(\gamma) * [\underline{n}] \qquad (2.1)$$

where γ is a time-varying angle whose rate of change is the orbital rate of the spacecraft. This orbiting frame traverses the nominal motion of the spacecraft. However, the actual motion of the spacecraft is a three-dimensional rotational departure from this nominal motion (see Fig. 3). Using the Euler angle parameterization once more, the satellite's departure motion may be specified by one of the qualifying sequences mentioned previously. Throughout this research, the 1-2-3 Euler angle set was used to parameterize the departure motion discussed above. Further, the departure motions about the sequenced axes are given names historically associated with aircraft motion: 1 - yaw (ψ), 2 - pitch (θ) and 3 - roll (ϕ). The projection of the body-fixed frame onto the orbiting frame is:

$$[\underline{b}] = DCM_3(\phi) * DCM_2(\theta) * DCM_1(\psi) * [\underline{o}]. \qquad (2.2)$$

which may be written in a further shorthand as:

$[\underline{b}] = [BO] * [\underline{o}]$ (2.3)

The matrix [BO] is a 3X3 array defined by the multiplication of the three 3X3 DCMs indicated and relults in the following:

$$[BO] = \begin{bmatrix} c\theta c\phi & c\phi s\theta s\psi + s\phi c\psi & -c\phi c\psi s\theta + s\psi s\phi \\ -c\theta s\phi & c\phi c\psi - s\phi s\theta s\psi & c\psi s\theta s\phi + s\psi c\phi \\ s\theta & -c\theta s\psi & c\psi c\theta \end{bmatrix}$$

Using the same shorthand scheme found in Eq. (2.3), Eq. (2.1) may be re-written as follows:

$[\underline{o}] = [ON] * [\underline{n}]$ (2.4)

The advantage of this shorthand becomes obvious as the following equation may be written:

$$[BN] = [BO] * [ON]$$

Thus the body axes are related to the inertial axes by:

$[\underline{b}] = [BN] * [\underline{n}] = [BO] * [ON] * [\underline{n}]$ (2.5)

where the arguments of the transformation matrix [BN] - namely ψ, θ, ϕ, and γ - are time-varying angles.

At this point, an explicit time-varying parameterization has been specified which uniquely describes the directions of the body-fixed axes and an arbitrarily chosen inertial reference frame. This relationship is easy to visualize and provides an efficient method of orienting the spacecraft relative to the earth.

2.2 Kinematics - Star Sensors: Since the assumption of a

rigid spacecraft is made, the last transformation (detailed above) allows the location of any point on the orbiting body relative to the inertial reference frame. The rigid-body assumption makes the absolute orientation of the spacecraft using on-board star sensors easier to describe mathematically in that the directions defined by the boresights (line-of-sight normal to the sensor plane) of each of the star sensors remain constant in body-fixed coordinates. For simplicity, two star sensors are assumed to be 90° apart and located 45° from the $\underline{b}_3$ axis in the $\underline{b}_2$-$\underline{b}_3$ plane. (The "left sensor" is 45° away from the positive $\underline{b}_3$ axis and is the result of a positive rotation about the $\underline{b}_1$ axis. The right sensor is similarly located on the opposite side of the $\underline{b}_3$ axis.)

According to this convention, the transformation matrices which locate the boresight directions relative to the body-fixed reference frame are as follows:

$$[RB] = \begin{bmatrix} 1 & 0 & 0 \\ 0 & c(45^{\circ}) & s(45^{\circ}) \\ 0 & -s(45^{\circ}) & c(45^{\circ}) \end{bmatrix} = [LB]^T \qquad (2.6)$$

This arrangement of sensors allows the spacecraft to sense a swath of stars on each side of its velocity vector (i.e. the $\underline{b}_3$ axis). The necessity of such redundancy becomes clear in Chapter 4.

2.3 Dynamics: The spacecraft that served as a model for this research is pictured in Fig. 2. In the spacecraft, it is assumed that three reaction wheels, momentum wheels, or control moment gyroscopes are oriented along the body-axes to admit control and stabilization of the attitude of the spacecraft. This attitude control is accomplished by changing the speed of the reaction wheels in order to transfer the distribution of the total momentum of the system among the body-fixed axes. Based on the principle that the time derivative of the system's angular momentum equals the external torque, the motion of the satellite is governed by a set of first-order differential equations. Mathematically, this may be written as Euler's equations:

$$\underline{L} = \dot{\underline{H}}$$

where $\underline{L}$ is the torque vector, $\underline{H}$ is the angular momentum vector, and the "dot" denotes an inertial time derivative. The components of the torque and angular momentum vectors are the magnitudes of torque and angular momentum about each of the body-fixed axes. If no momentum wheels exist, or if the wheels are locked, the vector equation above reduces to the standard form of Euler's equations for a rigid body. Various forms of the familiar equations may be found in any standard dynamics text (see Ref. 10 for further details on the derivation and several forms of Euler's equations).

Basically, the form of the spacecraft equation of motion is:

$$\dot{H}_i = f_i(\underline{\omega}, \dot{\underline{\omega}}, \underline{I}), \quad i=1,2,3$$

where: $\underline{I}$ is a vector containing the principal moments of inertia of the spacecraft, $\underline{\omega}$ is the angular velocity vector and f_i is a generally non linear relationship. The inertia of a rigid body is actually defined by a second-order tensor with three eigenvalues - the elements of the inertia vector.

The elements of $\underline{\omega}$ correspond to the angular velocity of the satellite projected onto the body-fixed reference frame. It is important to note that these elements are not the yaw, pitch, and roll angular rates, but that the latter rates may be obtained from the former by inverting a non linear, transcendental set of equations. However, since the body-fixed frame is usually a small angle departure from the orbital frame, these transcendental equations may be linearized by neglecting higher-order terms and approximating the trigonometric functions having these small arguments. The relsulting kinematic equations relating angular velocities to the yaw, pitch, and roll rates are:

$$\dot{\psi} = \omega_1 - \omega_o \phi \qquad (2.7a)$$

$$\dot{\theta} = \omega_2 - \omega_o \qquad (2.7b)$$

$$\dot{\phi} = \omega_3 + \omega_o \psi \qquad (2.7c)$$

where ω_0 is the orbital velocity - 2π /(orbital period). These equations must be integrated to determine the values of yaw, pitch and roll, which is the ultimate goal of attitude determination. The method of integration and necessary prior information is discussed in Chapter 4.

Thus, it is shown that angular velocity (and hence rates of yaw, pitch, and roll) are related to external moments and the assumed constant inertia properties of the spacecraft. Further, equations have been established showing that the attitude of the satellite may be adjusted by applying internal torques to the reaction wheels.

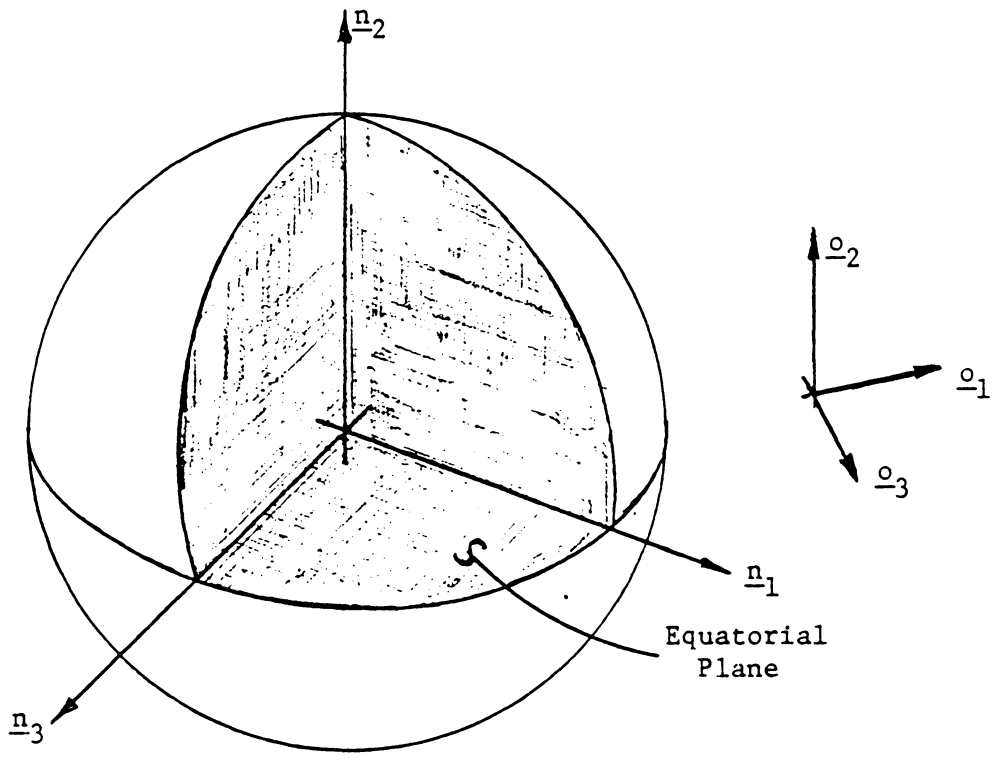

Figure 1 - Orientation of Reference Frames

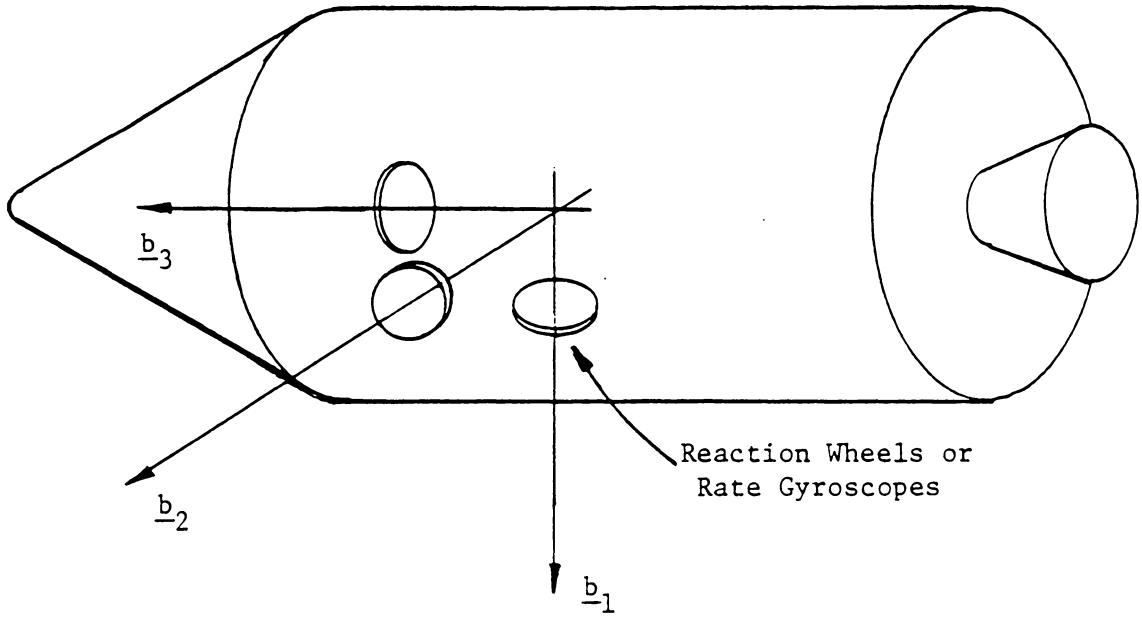

Figure 2 - Spacecraft Model

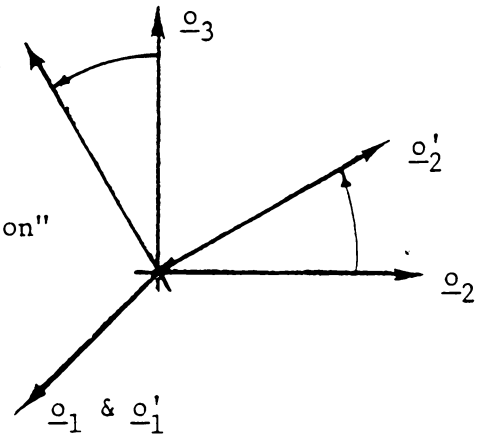

"1-Rotation"

Figure 3a

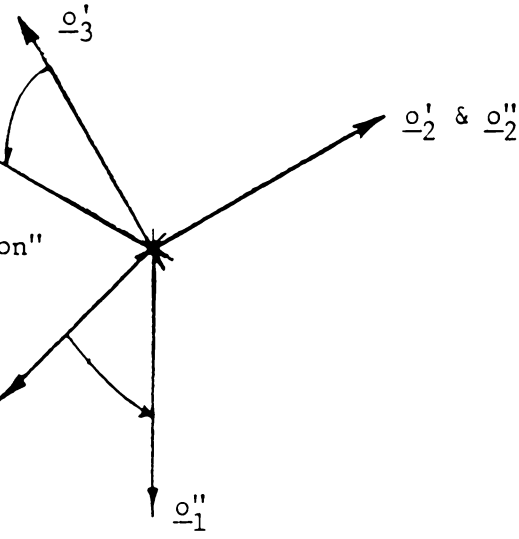

"2-Rotation"

Figure 3b

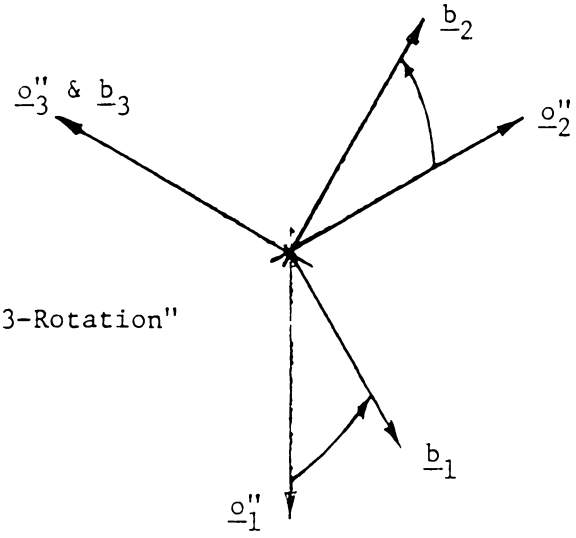

"3-Rotation"

Figure 3c

CHAPTER 3

RATE GYROSCOPE DATA SMOOTHING

3.0 Overview: This chapter discusses the method used to process the information received from satellite rate gyroscopes. Simply explained, coefficients are obtained for a Fourier Series that, when evaluated, yields zero residuals at all sample points. This series is successively deprived of high frequency contributions to yield a smooth approximation of original data that has the same residual variance that the manufacturer expects of the rate gyroscopes and the associated digitization of the analog output. The rationale and method of the fitting scheme are also presented.

The output from the smoothing segment of the rate gyroscope data processing sequence yields a time series approximation of rate gyroscope measurements that replaces the originally transmitted sequence of measurements. This replacement series is continuous and is a more reliable estimate of the true motion of the spacecraft in that the discrete, noisy rate gyroscope output is replaced by the smooth estimate. The degree of smoothing achieved is constrained to be consistent with the assumed known statistics of the rate gyroscope measurement errors.

3.1 Rate Gyroscope Data from the Satellite: On board any satellite utilizing strapdown navigational equipment, there exist at least three rate-measuring devices (i.e. gyroscopes) usually positioned orthogonally with respect to each other. Quite frequently, there are more than three rate gyroscopes to provide a redundancy of measurements enabling analysts to discover inconsistencies among the basic three rate gyroscope outputs. The redundancy provided by the extra rate sensors introduces extra computation in arriving at an improved estimate of angular rate about each of the three body axes. Since the general principles discussed in this chapter apply as a pre-processing of any rate gyroscope output, the simpler case of only three orthogonal rate gyroscopes will be considered here.

The raw data received from the rate gyroscopes on the satellite consist of electrical voltage pulses indicating, by frequency or amplitude modulation, the magnitude of the angular velocities sensed by the rate gyroscopes about each of the three body-fixed axes. The rate gyroscopes themselves may use any one of several different physical principles to determine the angular rates (see reference 2), but all types are subject to the same two types of errors - noise and drift. Noise is a random phenomenon occuring principally because of unpredictable electrical

and/or mechanical transients in sensing, digitizing and processing the information from each rate gyroscope. Drift (or bias) is an offsetting departure from the true angular velocity history. In a typical unclassified study of the errors associated with integrating rate gyroscopes, it was found that an inertial reference system (IRS) employing a single star sensor coupled with a triad of integrating rate gyroscopes feeding a Kalman filtering process yield a total inertial attitude error of less than 3.6 arc-sec (one sigma)[11]. Further, these studies also show that the above error sources (noise and drift) are the major contributors to this total error[1].

3.2 Smoothing Algorithm: In this section, a pre-processing algorithm is discussed which is applied to the sequence of raw rate gyroscope measurements. In the first step in the algorithm, coefficients are computed for a Fourier Series approximates the raw rate gyroscope data with zero residuals at every sample point. (For a complete discussion of the Fourier Series and applications thereof, see references 13 and 14.) Due to the nature of this type of series, a certain "characteristic time length" must be specified. Thus, the smoothing process discussed here is a batch algorithm as opposed to a sequential estimation process such as the Kalman filtering scheme. The process

of fitting a time series with a Fourier Series usually entails evaluating the standard integral equations to find the individual Fourier coefficients. Although that particular route may be taken, when certain conditions exist it is computationally easier to approach the job of finding these coefficients from a discrete least squares viewpoint. This is possible because in actuality the Fourier Series is the least squares estimate of a trigonometric curve-fit[12].

In order to see the Fourier Series as a standard least squares fitting process, it must be established that discrete evaluations of the familiar series may be written in the following form:

$$\underline{y} = [A]\underline{x}$$

In this form, as it relates to the evaluated Fourier Series, $\underline{y}$ is the value of the time series at each sample point, $\underline{x}$ is a vector of the Fourier coefficients a_i and b_j ($i=0,1,\ldots,N$ and $j=1,2,\ldots,N$), and [A] is a matrix defined as follows:

$$\begin{bmatrix} 1 & \cos\omega t_1 & \sin\omega t_1 & \cos 2\omega t_1 & \sin 2\omega t_1 & \ldots & \cos M\omega t_1 & \sin M\omega t_1 \\ 1 & \cos\omega t_2 & \sin\omega t_2 & \cos 2\omega t_2 & \sin 2\omega t_2 & \ldots & \cos M\omega t_2 & \sin M\omega t_2 \\ \cdot & \cdot & \cdot & \cdot & \cdot & \cdots & \cdot & \cdot \\ \cdot & \cdot & \cdot & \cdot & \cdot & \cdots & \cdot & \cdot \\ \cdot & \cdot & \cdot & \cdot & \cdot & \cdots & \cdot & \cdot \\ 1 & \cos\omega t_N & \sin\omega t_N & \cos 2\omega t_N & \sin 2\omega t_N & \ldots & \cos M\omega t_N & \sin M\omega t_N \end{bmatrix}$$

where $\omega = 2\pi/T$ (T is the "characteristic time length" described above), N is the number of points sampled, and M = 2N+1 for a complete series.

3.3 Fourier Coefficients by Least Squares: Although the principle of least squares is discussed further in the next chapter, the solution vector, whose elements are the required coefficients, in this case is obtained by a simple matrix inverse if the full series is desired. The task of obtaining the inverse is made easier by the fact that the sine and cosine are orthogonal functions with respect to a unity weight. For discrete sampling, this orthogonality does not hold for sample points arbitrarily placed in time. It can easily be verified however, that this orthogonality does hold for a uniform sampling, symmetric in time about t = T/2. Since the trigonometric functions possess this property in this case, the inverse of $([A]^T[A])$ is a diagonal matrix with the elements thereof equal to the sum of the squares of the elements in one column of [A]. The inverse of this diagonal matrix follows immediately and the solution for a typical element of $\underline{x}$, x_k $(k=1,2,\ldots,2N+1)$, may be written:

$$x_k = \frac{\sum_{j=1}^{N} y(t_j)p_k(t_j)}{\sum_{j=1}^{N} p_k^2(t_j)}$$

where $p_k(t_j)$ is a cosine or sine (depending on whether an a_i or b_j coefficient is sought) evaluated at a particular

frequency and time t_j. Due to the orthogonality of the cosine and sine basis functions with respect to the weight function of unity, the x_k are independent of each other, therefore adding or deleting terms in an incomplete Fourier Series does not change the remaining elements in the series.

3.4 Fourier Series Truncation Scheme: When the enitre series is evaluated, the raw rate gyroscope data is reproduced exactly at the sample points - noise included - but the purpose of this algorithm is to filter the noise from the rate gyroscope data. In order to eliminate or reduce the unwanted noise, assumptions must be introduced concerning the statistical characteristics of the noise.

Intuitively, as a spacecraft changes attitude in any way, the motion is continuous and, with the exception of the oscillatory, high-frequency vibration transients induced by the error of the rigid-body assumption, devoid of the small, random spikes present in a typical rate gyroscope record. Since these low-amplitude discontinuities in angular velocity are not indicative of what is reasonably expected of the motions actually executed, it is reasonable to seek a smooth approximation to replace the raw data. The nature of these undesirable

discontinuities suggests that they could be interpreted as measurement noise. Unfortunately, there is no rigorous way to uncover the true motion exactly from a noisy signal. The spikes in the rate gyroscope record which are assumed to be associated with random noise may be eliminated to an acceptable degree of approximation by omitting the evaluation of the coefficients associated with frequencies above a certain threshold.

The relative accuracy of a series with fewer coefficients than a full Fourier Series is quantified by the statistics of the residuals between the transmitted time series and the inexact estimate of that series. The absolute accuracy of the approximation strategy can only be evaluated based upon simulation studies where the underlying true motion is known.

3.5 Truncation Criterion: With the method of singling-out high frequency contributions available, the algorithm must now incorporate the expected error of the rate gyroscopes into the smoothing process. The unique feature of the method being discussed here is the fact that the final estimate of the angular velocity of the spacecraft at any time in the batch record is a statistically consistent, smooth approximation of the actual rate gyroscope data: the variance in the residuals constrained to equal the

variance of the rate measurement errors expected by analysis of the rate gyroscopes and the analog-digital conversion process. The smoothing approach uses this fact as a stopping criterion for the truncation of coefficients in the series approximations.

The standard method of acquiring residual statistics is to evaluate the partial Fourier Series at each point in time where data is available and compute the difference between these curves. This method proved to be prohibitively expensive, even with a large mainframe computer. To bring the task within reach, Parseval's equality and Bessel's inequality are incorporated into the algorithm. In short, the combination of these mathematical expressions states that the sum-square of the residuals over the entire period of time considered will always be less than or equal to the sum-square of the coefficients not included when computing the current partial Fourier Series. A logical "trap" is therefore placed in the program to find the number of coefficients that may be deleted before the sum-square of those coefficients exceeds the rate gyroscope variance. (Recall here that the variance of the residuals is equal to the sum-square of the residuals less the mean residual squared. Thus the implicit assumption is made that the mean residual is negligible - a good assumption when using the least squares

method.)

Once the series fits the data to barely within the rate gyroscope variance (as decided by the above logic), control in the program is passed to the standard methods of evaluating the statistics of the residuals. In this segment of the smoothing process, the series is evaluated, the residuals and the statistics of the residuals are found by standard formulas. If the present residual variance is smaller than the rate gyroscope variance, the previous fit is recalled and accepted as fitting the original data as accurately as the rate gyroscope can measure. If the variance is still greater than the rate gyroscope variance, the next pair of Fourier coefficients is restored to the truncated series and the process repeats itself. When this segment of the program is completed, an estimate of the time series exists, based on the final partial Fourier Series, that fits the original time series to the same accuracy expected of the rate gyroscope and does not include or greatly reduces the high frequency elements predominantly associated with random noise in the measurements.

At this point, the raw rate gyroscope time series data has been approximated in a manner consistent with the expected accuracy of the gyroscopic instrumentation. The entire smoothing process is completed when the data

obtained from all rate gyroscopes has been fit in the manner described in this chapter.

CHAPTER 4

PARAMETER ESTIMATION

4.0 Overview: In Chapter 2, the integration of the kinematic relationships was discussed along with the rate gyroscope error of bias (drift). In order to integrate the kinematic equations, initial conditions are needed, but the subject of determining these values was not treated. A method was presented whereby unwanted rate gyroscope noise could be filtered out, but no procedure was given to remove the gyroscope bias errors. In Chapter 4, the algorithm used for determining the quantities above is presented. This algorithm involves estimating these values initially and correcting them in an iterative fashion until convergence is achieved using the method of Gaussian Least Squares Differential Correction.

In addition to estimating the six parameters listed above, a method is given to extend this iterative procedure to other poorly known values such as interlock angles between the left and right star sensors. Certain restrictions apply to the set of the parameters that may be estimated in this manner. These restrictions are presented and explained.

As a matter of completeness, the collinearity equations and their uses are presented and discussed in a

limited fashion.

4.1 Gaussian Least Squares Differential Correction Scheme:

In this section, a familiarity with the fundamental concepts and procedures of the standard method of least squares will be assumed. This method of fitting redundant data so that the square error of the approximation is minimized is discussed and derived in detail in Refs. 15 and 16. Using the standard notation found in these references, the coefficient matrix of a linear set of equations is denoted [B], the unknown quantities to be estimated are placed in vector form and collectively denoted $\underline{x}$ and the right-side vector of constants is denoted $\underline{f}$. The least squares solution to the redundant matrix equation $[B]\underline{x} = \underline{f}$ (where all measurements have equal reliability or weights) is:

$$\underline{x} = ([B]^T[B])^{-1}([B]^T\underline{f})$$

where the superscripts T and -1 signify the matrix transpose and inverse, respectively. The above solution minimizes the quantity $\underline{e}^T\underline{e}$, where $\underline{e} = \underline{f} - [B]\underline{x}$ (the sum of the squared residuals of the approximation).

If the system of non linear equations possesses a linear coefficient matrix that is dependent on the solution vector ($\underline{x}$) of the estimation, the solution procedure changes: instead of solving directly for the solution

vector, a differential correction vector, $\underline{dx}$, is sought. The solution equation then becomes:

$$\underline{dx} = ([B]^T[B])^{-1}([B]\underline{df})$$

where [B] is now a matrix of locally evaluated partial derivatives, which is dependent on the solution vector $\underline{x}$, and $\underline{df}$ represents a difference in the constant vector (locally evaluated residuals between measured and computed values).

As mentioned before, the parameters to be estimated are the initial values for ψ, θ, and ϕ, and the rate gyroscope biases about each of the three body-fixed axes denoted b_i (i=1, 2, 3). The differential corrections to these six values comprise the vector of unknowns, $\underline{dx}$. The vector $\underline{df}$ contains residuals of the x and y coordinates on the star sensor focal plane. The geometrical projection of inertial star position onto the x-y plane is discussed in further detail in the next section.

4.2 Collinearity Equations: The collinearity equations are in wide use in the branch of surveying called photogrammetry. Photogrammetry concerns itself with relating measurements on photographs taken from an aircraft or spacecraft (either singly or in stereo pairs) to features and/or accurately determined points on the earth's surface. The metric camera used to take these pictures is

special in that the focal length and lens distortion are precisely calibrated and the film plane is "flat" to within very fine tolerances. In the case at hand, the "cameras" on the spacecraft are the two star sensors which are 10mm square and assumed to possess the same qualities as metric cameras. The x and y coordinates on a photograph and on the star sensor plane are taken from the center point and are defined by the stellar collinearity equations[12]:

$$x = -f \frac{l_1C_{11} + l_2C_{12} + l_3C_{13}}{l_1C_{31} + l_2C_{32} + l_3C_{33}}$$

$$y = -f \frac{l_1C_{21} + l_2C_{22} + l_3C_{23}}{l_1C_{31} + l_2C_{32} + l_3C_{33}}$$

$$z = -f$$

where l_i (i=1, 2, 3) is an inertial position vector to a particular star from the inertial origin, C_{ij} is the DCM that relates the star sensor plane to the inertial coordinate system, and f is the focal length of the lens on the star sensor. The z-coordinate is always -f because of the assumed position of the origin of the sensor coordinate system - at the perspective center of the lens of the star sensor.

The cataloging and access of the inertial position vectors to several thousand stars are significant tasks. However, several star catalogs and access schemes are available which adequately treat these subjects[17].

4.3 Kinematic Equations Revisited: The kinematic equations presented in chapter 2 may be written in matrix form as:

$$\dot{\underline{X}} = [A]\underline{X} + \underline{F}$$

where [A] is a coefficient matrix, and $\underline{F}$ is a 6X1 vector, consistent with the matrix dimensions of the rest of the equation. The individual elements of the above equation are given as follows:

$$\underline{X} = \begin{Bmatrix} \psi \\ \theta \\ \phi \\ b_1 \\ b_2 \\ b_3 \end{Bmatrix}, \quad [A] = \begin{bmatrix} 0 & 0 & -\omega_0 & 1 & 0 & 0 \\ 0 & 0 & 0 & 0 & 1 & 0 \\ \omega_0 & 0 & 0 & 0 & 0 & 1 \\ 0 & 0 & 0 & 0 & 0 & 0 \\ 0 & 0 & 0 & 0 & 0 & 0 \\ 0 & 0 & 0 & 0 & 0 & 0 \end{bmatrix}, \quad \underline{F} = \begin{Bmatrix} \omega_1 \\ \omega_2 - \omega_0 \\ \omega_3 \\ 0 \\ 0 \\ 0 \end{Bmatrix}$$

The above system may be partitioned into two systems of order 3 where:

$$[A] = \begin{bmatrix} [A_{11}] & [I] \\ [0] & [0] \end{bmatrix}$$

where [I] is the identity matrix and [0] is a matrix fully populated by zeros.

If $\underline{X}$ is given to be a vector of state variables, the following state-transition relations exist (see Ref. 18):

$\underline{X}(t) = [\Phi(t,t_0)]\underline{X}(t_0)$ and $[\dot{\Phi}(t,t_0)] = [A][\Phi(t,t_0)]$ (4.1a,b)

where $[\Phi(t,t_0)]$ is known as the state-transition matrix. $[\Phi(t,t_0)]$ may be partitioned in a similar manner to the way [A] was partitioned:

$$[\Phi(t,t_0)] = \begin{bmatrix} [\Phi_{11}] & [\Phi_{12}] \\ [\Phi_{21}] & [\Phi_{22}] \end{bmatrix}$$

The above partitioning allows an intuitive interpretation of Eqs. 4.1a and b: Since the rate gyroscope biases are assumed to be constant over the batch of measurements considered, it is obvious that

$$[\Phi_{21}] = [0] \text{ and } [\Phi_{22}] = [I]$$

The non-trivial differential equations resulting from the above partitionings are:

$$[\dot{\Phi}_{11}] = [A_{11}][\Phi_{11}] \text{ and} \quad (4.2)$$

$$[\dot{\Phi}_{12}] = [A_{11}][\Phi_{12}] + [I] \quad (4.3)$$

The initial conditions for $[\Phi_{11}]$ are $[\Phi_{11}(t_0,t_0)] = [I]$. These conditions are intuitively obvious when the meaning of the state-transition matrix is considered. The solution of Eq. (4.2) is found by the standard method of solution for linear, homogeneous differential equations and in this case the solution is:

$$e^{[A]T} = \begin{bmatrix} c(\omega_0 T) & 0 & -s(\omega_0 T) \\ 0 & 1 & 0 \\ s(\omega_0 T) & 0 & c(\omega_0 T) \end{bmatrix} \tag{4.4}$$

where $T = t - t_0$. Hereinafter the elements of this solution matrix will be denoted H_{ij} and it should be noted that these elements represent the sensitivities of yaw, pitch, and roll at any time after t_0 (i=1, 2, 3) with respect to the values of these same parameters at time t_0 (j=1, 2, 3). By inspection, the constant that should precede the solution expression (in accordance with differential equation theory) is equal to one in order to satisfy the initial conditions (an identity matrix for $[\Phi]$). This same solution matrix could also have been derived by a careful consideration of the meanings of the individual elements given above.

The homogeneous solution to Eq. (4.3) is the same as the complete solution to Eq. (4.2), but the particular solution must also be found. The method of variation of parameters is utilized here to obtain a particular solution to the equation at hand: If the constants involved in the homogeneous solution are not "constant" but are allowed to vary with time in order to satisfy the inhomogeneity of the equation exactly, then:

$$\dot{[\Phi_{12}]} = \dot{[P]}[H] + [P]\dot{[H]} \tag{4.4}$$

where [H] was defined previously and [P] is the particular solution to Eq. (4.3). If Eqs. (4.3) and (4.4) are combined,

$$\dot{[P]} = [H]^{-1}[I] = [H]^{T} \tag{4.5}$$

due to the orthogonality of [H]. Eq. (4.5) may be integrated and subjected to the initial conditions on $[\Phi_{12}]$ to yield the final equation:

$$\omega_0[\Phi_{12}] = \begin{bmatrix} s\gamma & 0 & c\gamma - 1 \\ 0 & \gamma & 0 \\ 1 - c\gamma & 0 & s\gamma \end{bmatrix} \tag{4.6}$$

where γ is $\omega_0 T$.

Now that $[\Phi_{ij}]$ (i and j=1, 2) are defined and/or deduced, the entire state-transition matrix is known. This means that the sensitivity of any element of the state vector to the initial value of the same or any other element of the state vector is known. This information will be used in the next section to construct the sensitivity matrix [B] discussed earlier.

4.4 Image Measurement Sensitivity Matrix: As stated earlier, the sensitivity matrix [B] is composed of partial deriviatives of the elements of df with respect to the elements of dx. To find these derivatives explicitly, a triple sum must be evaluated for each element in [B]. This

summation process is a consequence of implementing the chain rule of differentiation and are as follows (the 1 subscript denotes a particular element of the vector X):

$$\frac{\partial x_R}{\partial X_1} = \sum_{i}^{(i=1,3)} \sum_{j=1}^{3} \sum_{k=1}^{3} \frac{\partial x_R}{\partial RN_{ij}} \frac{\partial RN_{ij}}{\partial q_k} \frac{\partial q_k}{\partial X_1}$$

$$\frac{\partial y_R}{\partial X_1} = \sum_{i}^{(i=2,3)} \sum_{j=1}^{3} \sum_{k=1}^{3} \frac{\partial y_R}{\partial RN_{ij}} \frac{\partial RN_{ij}}{\partial q_k} \frac{\partial q_k}{\partial X_1}$$

$$\frac{\partial x_L}{\partial X_1} = \sum_{i}^{(i=1,3)} \sum_{j=1}^{3} \sum_{k=1}^{3} \frac{\partial x_L}{\partial LN_{ij}} \frac{\partial LN_{ij}}{\partial q_k} \frac{\partial q_k}{\partial X_1}$$

$$\frac{\partial y_L}{\partial X_1} = \sum_{i}^{(i=2,3)} \sum_{j=1}^{3} \sum_{k=1}^{3} \frac{\partial y_L}{\partial LN_{ij}} \frac{\partial LN_{ij}}{\partial q_k} \frac{\partial q_k}{\partial X_1}$$

where x_R, y_R, x_L, and y_L are the x and y coordinates on the right and left star sensors respectively, [RN] and [LN] are the transformation matrices from the right and left star sensor coordinate system to the inertial system respectively, and q_k denotes the value of yaw, pitch, and roll corresponding to k=1, 2, 3. The transformation matrices and the values of the angular rates must be evaluated at the time the star is sensed at the x and y coordinate specified. Note that in order to evaluate the elements of [B], because of the dependence on [RN] or [LN]

evaluated at the time of a star hit, the kinematic equations must be integrated. This is accomplished using a four-step Runge-Kutta algorithm, an explanation of which may be found in most numerical methods texts.

Although the above equations appear to be quite formidable, the task of evaluating them is simplified by the frequent appearance of zeros in the factors of the summations. For example, the last factor in each summation expression is simply a particular element of the state-transition matrix - most of which are zero. The middle factor is found by a straightforward application of differentiation to the transformation matrices and the first factor is found by an application of the chain rule of differentiation to the collinearity equations - a straightforward process, but messy.

Using the partial derivatives described above, [B] is defined fully and will have dimensions (2nX6) where n is the number of star shots recorded.

4.5 Iteration Procedure and Stopping Criterion: To begin this correction scheme, initial estimates for all parameters are necessary. Since the procedure outlined to correct these estimates has been proven over the years to be fairly robust, an acceptable estimate for this initialization is zero for all elements in $\underline{X}$. With this

first estimate, [B] may be evaluated by carrying out the summations described in the previous section.

Next, the "constant" vector df must be evaluated. For this phase of the process, discrepancies between the measured star sensor x and y coordinates and the x and y coordinates calculated by substitution into the collinearity equations are found. These discrepancies become elements of df. It is important to note at this point that if six parameters are to be estimated, at least four sets coordinate residuals must exist, implying that the iteration procedure cannot be implemented until four star shots are registered. This assumption allows the use of the Gaussian Least Squares Differential Correction procedure.

If more parameters are to be estimated, more star hits must be registered and [B] must be expanded using the same equations as before - evaluated at additional times. The other quantities that are to be estimated, however, must involve the inertial positioning of the spacecraft. The additional parameters must also have the capability of being determined by resolving the discrepancy between measured values and values computed from an appropriate mathematical model. Finally, the set of estimated parameters must be "observable" - i.e., the columns of [B] must locally be non-zero and linearly independent. One

important set of geometric parameters is the three interlock angles between the rate gyroscope axes and the star sensor coordinate systems, but these have been found to be unobservable. The interlock angles between the two star sensors are observable with the angle between the boresights being most accurately determined[19].

Theoretically, this procedure would keep iterating by finding a solution vector, evaluating [B] and df, finding another solution, etc. In order to halt the iteration process, a comparison is made between the sum-square of part of the present differential correction vector and the previous value of the same. It is shown in various texts on the least squares method that the relative error between successive differential corrections is a reliable basis for a stopping criterion. The measure used in this program is a sum-square of the elements of the differential correction vector. However, in the case of an unweighted adjustment, the corrections to the initial values of the angles overly dominate a sum-square of the entire vector and lead the algorithm to an erroneous conclusion concerning which iteration satisfactorily ends the program. One solution to the problem is to introduce weights into the relative error norm that reflect the incompatibility of size and units in the elements of the differential correction vector. Alternatively, it was observed that convergence was

sufficiently reliable when only the differential corrections to the biases were included in the relative error norm. This partial sum-square is used in the program to provide a simple and reliable stopping criterion.

CHAPTER 5

NUMERICAL EXAMPLES

5.0 Overview: Thus far in this thesis, a method has been presented to smooth raw rate gyroscope data thereby reducing "spike discrepancies" which are associated with noise and other high frequency contributions to the record. Further, the method of least squares was suggested to determine rate gyroscope biases and the initial conditions on each of the three angles used to parameterize the motion of an orbiting object. In this chapter, four numerical examples are presented where the methods described earlier are used. In the first example, simple motions about each of the three body-fixed axes are generated, smoothed and analyzed. The second simulation is more indicative of actual rate gyroscope output and as such is considerably more complicated than the first. Example 3 is generated with a large amount of noise introduced to the angular velocity measurements and Example 4 demonstrates the performance of the algorithm under precise pointing conditions.

In each of the examples, several figures are given. About each of the three body-fixed axes, the true attitude history and angular velocity history is plotted against time. In addition, and also for each of the three axes,

the folllowing residual plots are made: the true attitude minus the final estimated attitude, the true angular velocity minus the smoothed angular velocity and the raw rate gyroscope data minus the smoothed estimate of the angular velocity history. In the interest of clarity, the graphs mentioned above do not span the entire simulation period of 25 seconds. The graphs only encompass the first 6.4 seconds of the simulation, representing 256 data points sampled at 40 times per second.

In simulating the stellar data for all examples, star hits were assumed to occur every 2 seconds on alternating star sensors, beginning with the right sensor at the initial time. The true x and y coordinates of the line-of-sight vector on the sensor plane were given by a random number generator multiplying the assumed dimension of the sensor plane (5 mm square). To create a star catalog, these coordinates were then transformed into an inertial direction vector. By creating a star catalog, the separate issues of star identification interfacing with existing star catalogs were avoided. Gaussian noise with a magnitude of 1 micrometer (3-sigma) was then added to the measured coordinates by calling the same random number generator.

The orbital rate used in the calculation of all angular velocity histories was based on an assumed orbital

period of 90 minutes and for each of the examples discussed here, the following biases were added to the angular velocity measurements: to the $\underline{b}_1$ component, the bias added was 1.0×10^{-5}, to the $\underline{b}_2$ component, -1.2×10^{-5} was added and to the $\underline{b}_3$ component, 9.7×10^{-6} (all in radians/second). The magnitudes of the bias and noise added to the angular velocity measurements were selected based on typical values reported in Refs. 2, 4, 5, and 7.

Residual plots for one example of interest that are not included here represent a situation likely to be encountered in practice: A rather complicated angular motion wherein the noise on the simulated rate gyroscope measurements was two orders of magnitude smaller than that described above (i.e. better than 1 arc-second per hour accuracy, 1-sigma). In this example, no coefficients could be deleted in the angular velocity smoothing routine if the final estimate was to remain consistent with the statistics of the rate gyroscope errors. Deleting the highest frequency terms resulted in a residual variance larger than the rate gyroscope variance. This situation will always arise for sufficiently small noise, but the likelihood of this condition also depends on the high frequency content of the motion and the overall signal to noise ratio.

5.1 Example 1 - Low Frequency Motion: In the simplest

motion considered in this thesis, two comparatively low frequencies (and a random phase shift) became the arguments of the sine function to generate the true angular history. These frequencies are given, along with the amplitudes of the corresponding sine waves, in Table 1. Closed-form differentiation yielded the angular rates and the kinematic equations given in chapter 2 gave the true angular velocity histories. These true histories were then corrupted by the biases mentioned above and by gaussian noise with a zero mean and a 5.0×10^{-6} rad./sec. standard deviation. (This standard deviation corresponds to approximately 1 deg./hour of rate gyroscope error.)

The true and estimated initial values of the attitude angles and gyroscope biases are summarized in Table 2. In this table, I.C. denotes the initial value of the angle in question and # Coeff. Reqd. is the number of coefficients that were required to fit the raw data to an accuracy consistent with the rate gyroscope noise statistics. (The maximum number of coefficients allowed to fit 1000 data points is 500.)

The residual plots described above for Example 1 are given in Figs. 4, 5, 6, 7, and 8. In Figs. 4 and 5, it is seen that the simulated motion is not extremely "busy", but Table 2 indicates that a significant number of coefficients was required to adequately fit the raw data. Many terms

were required in the estimate because of the initial and final discontinuities and the random phase shift introduced into the attitude history, and because the frequencies used in the simulation are not even multiples of the arguments in the Fourier Series approximation. Note also that the residuals (Figs. 6, 7, and 8) exhibit a decaying periodic behavior. The periodicity of the residuals is due to the fact that a periodic function generated the signal with a certain frequency content and a "less-than-exact" representation with a differing frequency content was used in the approximation. The difference in frequency contents gives rise to the periodic error (analogous to "beats" in physics applications involving acoustics).

The apparent decaying nature of the residual curve is misleading. This behavior is present, however, only during the first and last segments of the estimated angular velocity history. It is due to the fact that the Fourier Series expects an infinite duplication of everything inside the "characteristic time length" (or period) specified with no discontinuities at the point where one period ends and another begins (i.e., the endpoints of the angular velocity batch). The Fourier Series cannot efficiently represent the sharp "jump" introduced at the initial and final points of the data set (see any text dealing with the Fourier Series and Gibb's phenomenon). In an angular velocity

history, such discontinuities can only be avoided if every component of the record ended at the same point it began, with the same slope at the beginning and end as well. This type of care was not exercised because a similar situation cannot be expected to occur in actual rate gyroscope records. Gibb's phenomenon is well-documented and there is no known cure, except to generate mirror-image data to the right and left of the actual data and "window" the time region of interest after fitting both the actual and mirrored samples.

Table 1 - Frequencies Present in Attitude History (Ex. 1)

Freq. [cps]	Amp. [rad]
0.08333	1.57×10^{-3}
0.01667	5.84×10^{-3}

Table 2 - Comparison of Results (Ex. 1)

Axis	Quantity	Truth	Estimate
1	I.C.	0.25897×10^{-2}	0.25919×10^{-2}
	Bias	0.10000×10^{-4}	0.10161×10^{-4}
	# Coeff. Reqd.		168
2	I.C.	-0.41715×10^{-3}	-0.41588×10^{-3}
	Bias	-0.12000×10^{-4}	-0.11906×10^{-4}
	# Coeff. Reqd.		249
3	I.C.	0.44791×10^{-2}	0.44786×10^{-2}
	Bias	0.97000×10^{-5}	0.98073×10^{-5}
	# Coeff. Reqd.		335

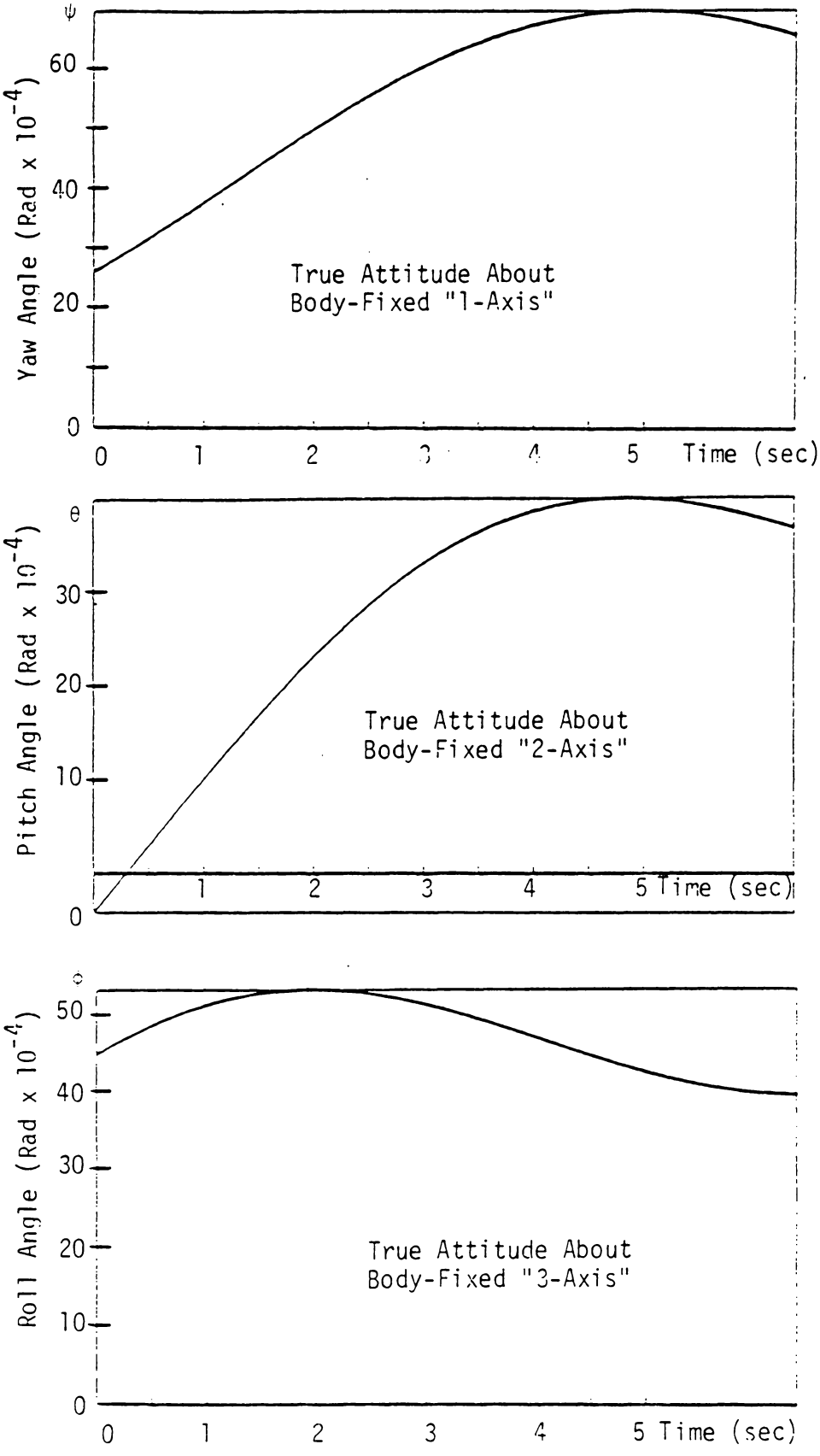

Figure 4 -. True Attitude History (Ex. 1)

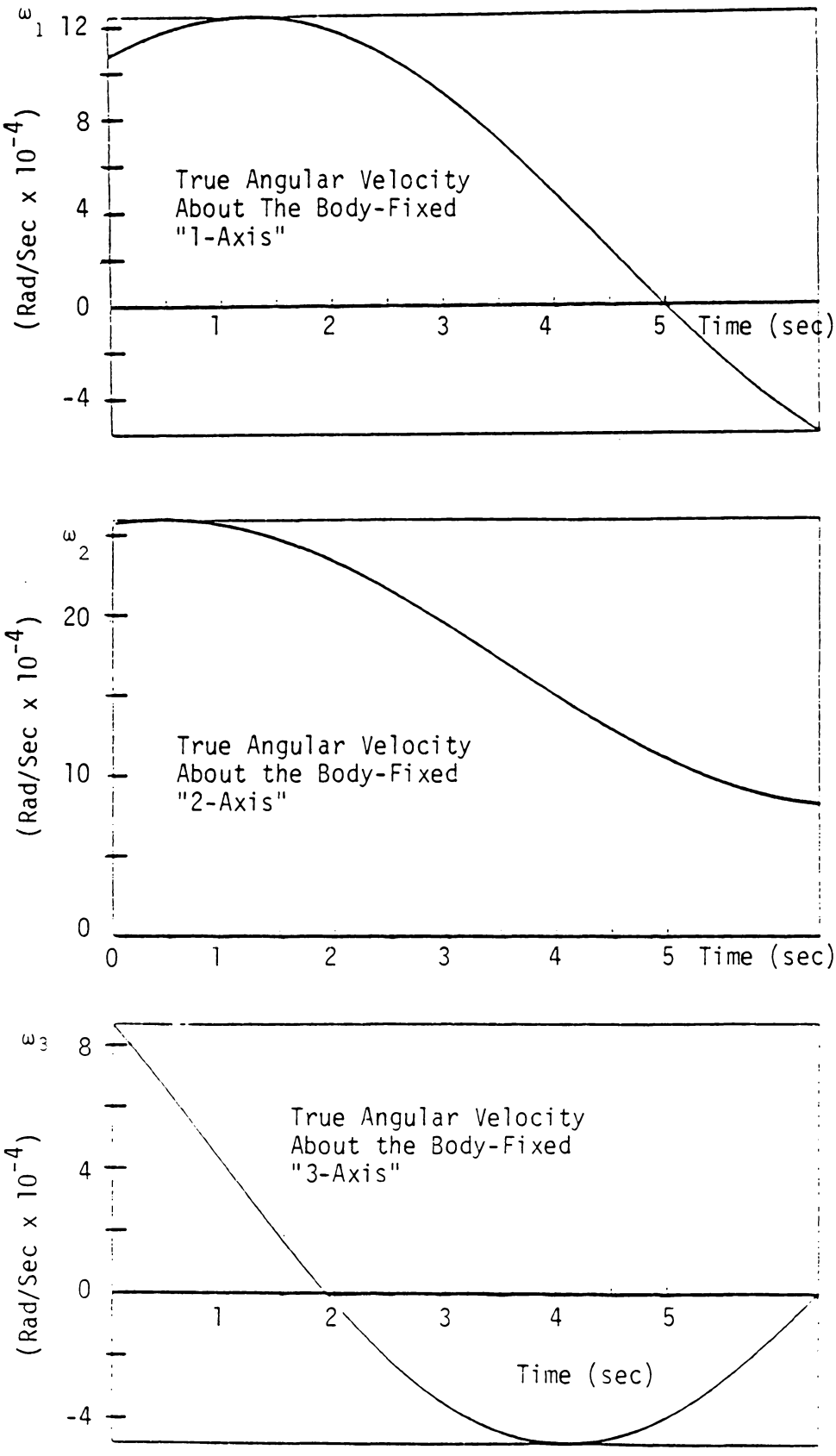

Figure 5 - True Angular Velocity History (Ex. 1)

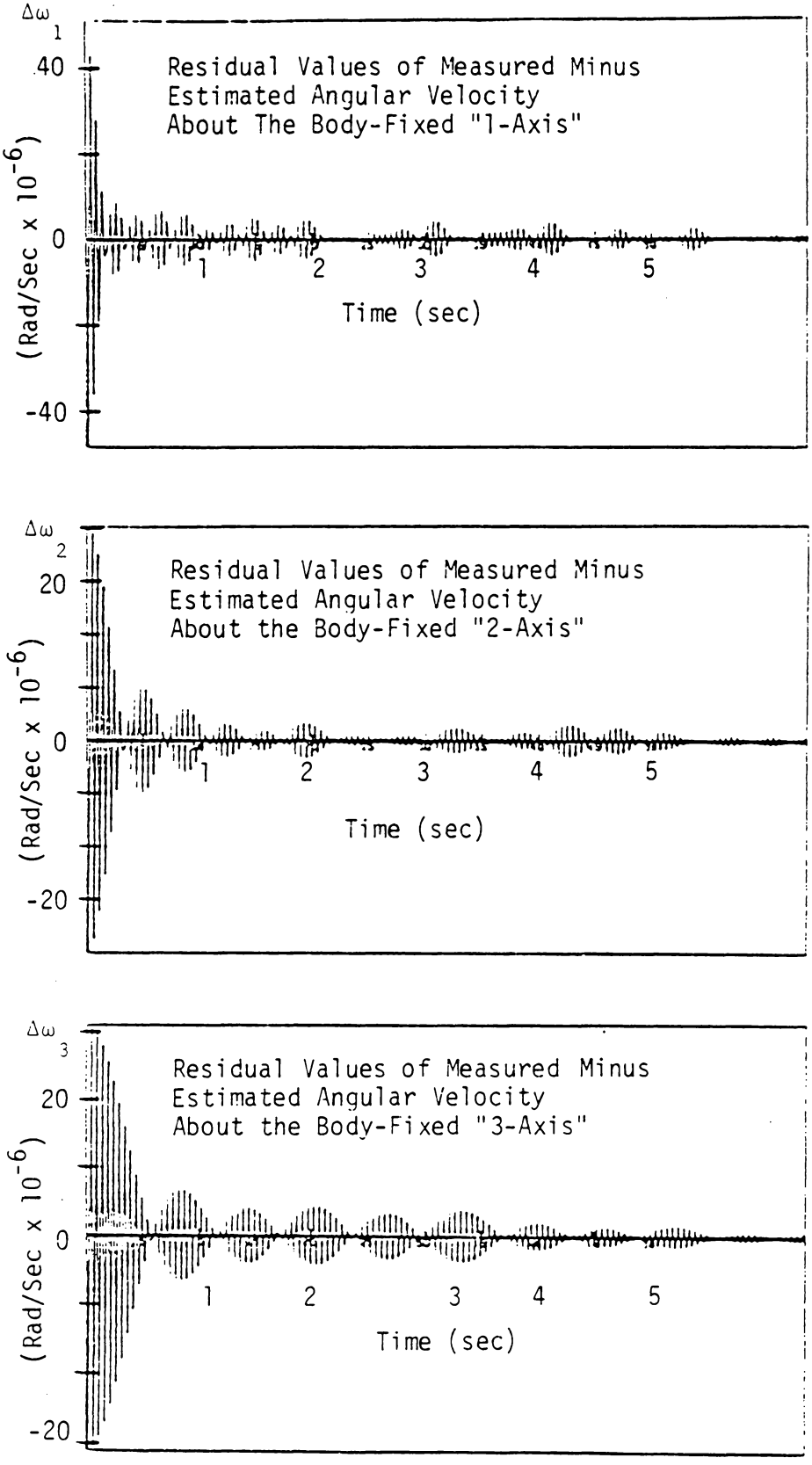

Figure 6 - Measured Minus Estimated Angular Velocity Residuals (Ex. 1)

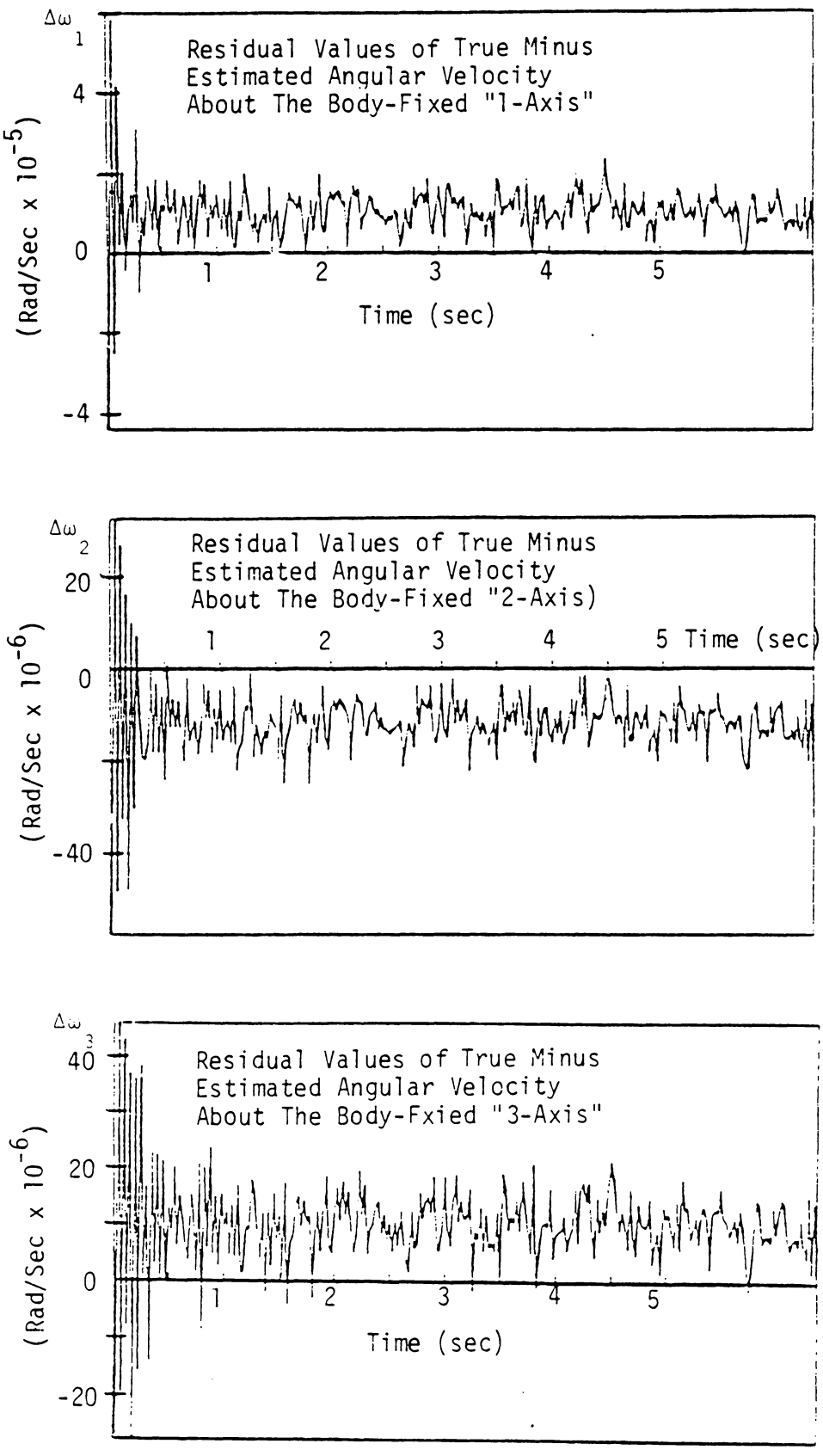

Figure 7 - True Minus Estimated Angular Velocity Residuals (Ex. 1)

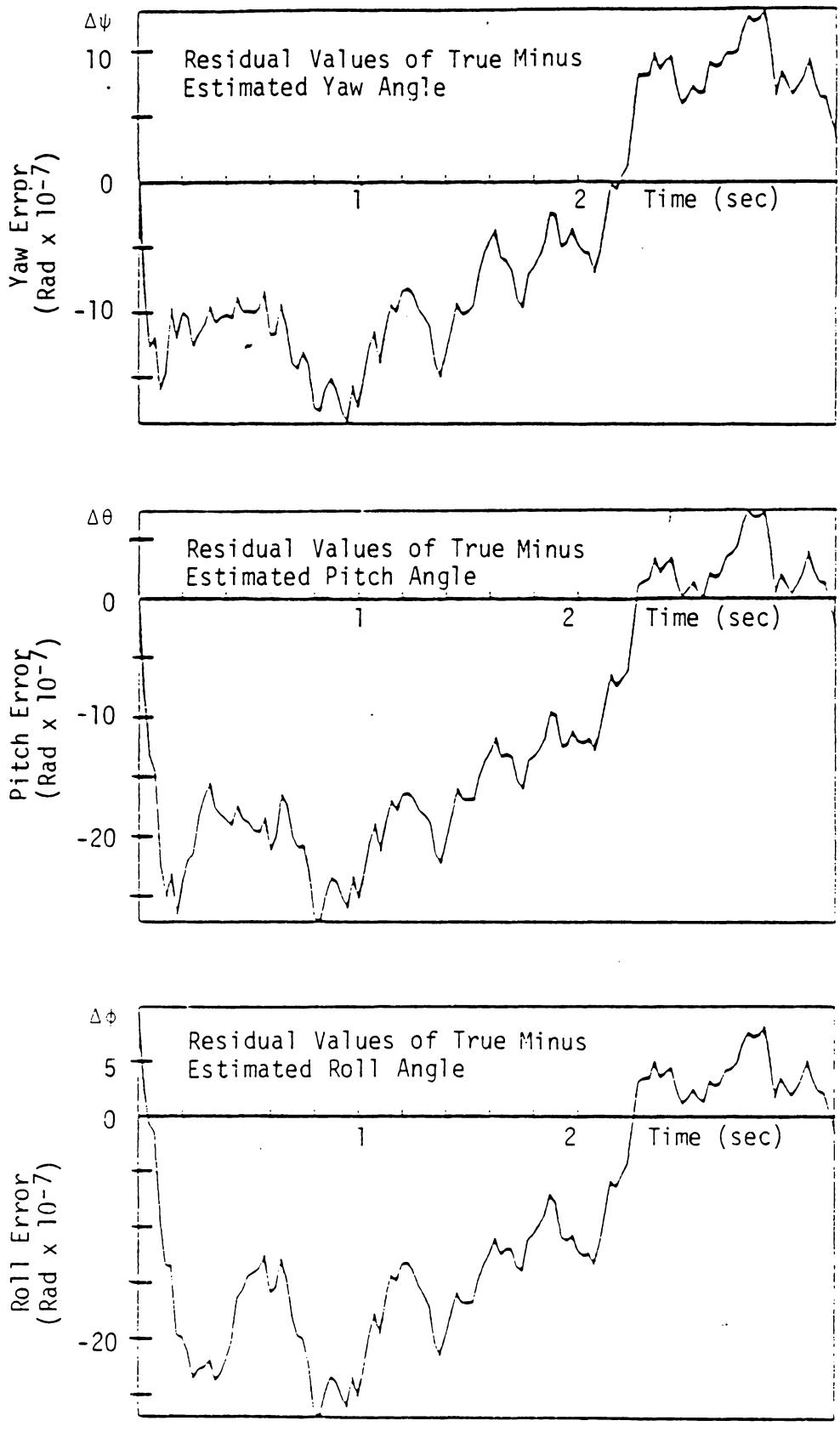

Figure 8 - True Minus Estimated Attitude Residuals (Ex. 1)

5.2 Example 2 - Combined High and Low Frequency Motion:

The second example presented and discussed here is different from the first in complexity only. Table 3 reveals that more frequencies were utilized in constructing the attitude history and thus the figures representing true attitude and angular velocity appear much more "busy" than the corresponding figures in Example 1. The biases mentioned earlier were added to the true angular velocity histories which were computed analogously to example 1. Noise with zero mean and a standard deviation of 5.0×10^{-6} radians/second was then superimposed on the signal. Figs. 9, 10, 11, 12, and 13 show the simulated truth model and residual quantities discussed in the overview and Table 4 summarizes the results of the adjustment of 1000 data points (and therefore 500 possible coefficients in the approximation process).

The comments and observations made in the previous section are equally applicable to the results presented in this section.

Table 3 - Frequencies Present in Attitude History (Exs. 2 and 3)

Freq. [cps]	Amp. [rad]
8.00000	5.25×10^{-5}
5.00000	2.17×10^{-4}
3.00000	1.05×10^{-4}
1.00000	3.14×10^{-4}
0.50000	3.93×10^{-4}
0.25000	1.05×10^{-3}
0.20000	1.05×10^{-3}
0.08333	1.57×10^{-3}
0.01667	5.84×10^{-3}

Table 4 - Comparison of Results (Ex. 2)

Axis	Quantity	Truth	Estimate
1	I.C.	0.16072×10^{-2}	0.16025×10^{-2}
	Bias	0.10000×10^{-4}	0.10049×10^{-4}
	# Coeff. Reqd.		472
2	I.C.	0.64963×10^{-3}	0.65296×10^{-3}
	Bias	-0.12000×10^{-4}	-0.11945×10^{-4}
	# Coeff. Reqd.		373
3	I.C.	0.43527×10^{-2}	0.43479×10^{-2}
	Bias	0.97000×10^{-5}	0.97821×10^{-5}
	# Coeff. Reqd.		467

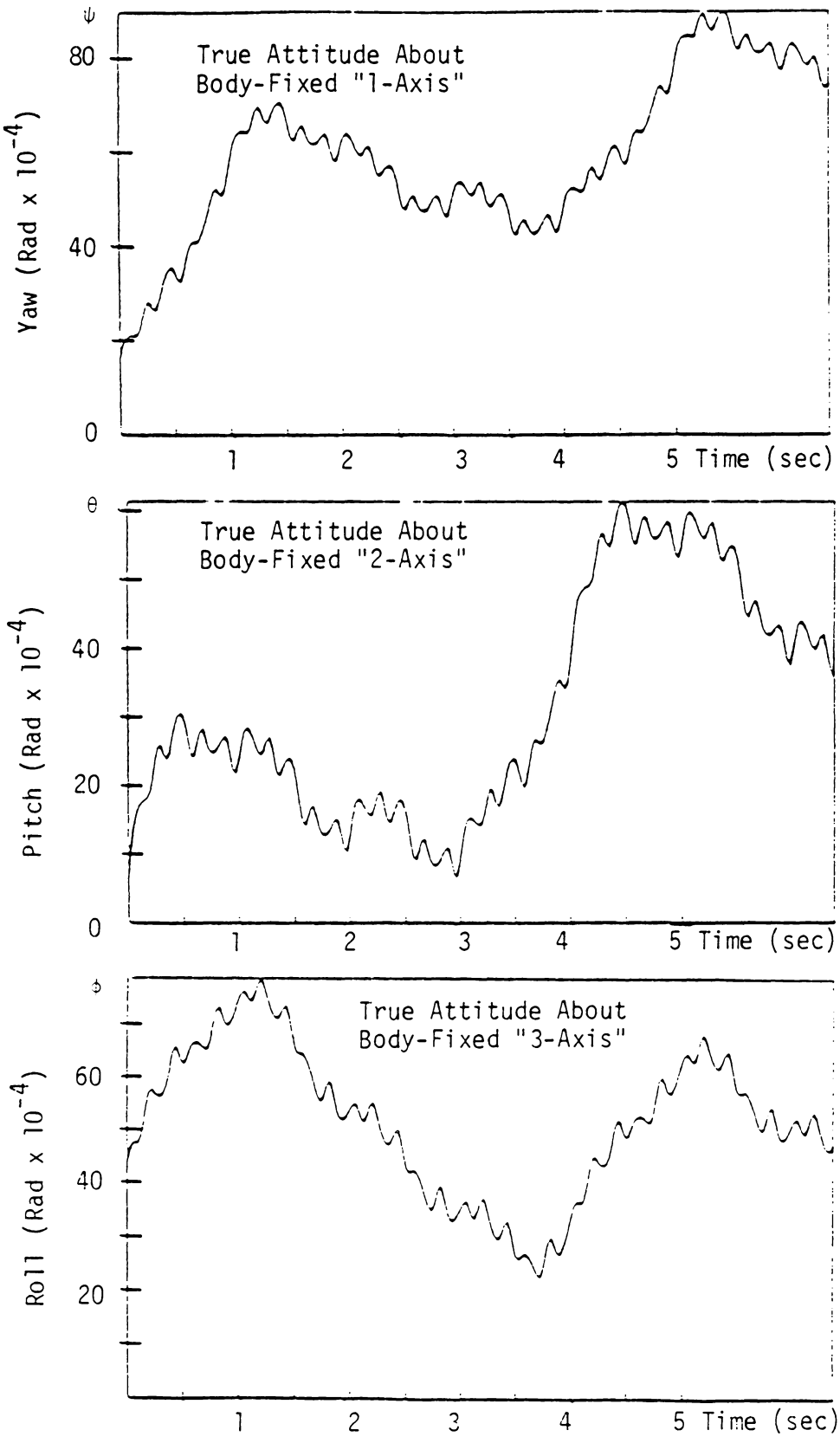

Figure 9 - True Attitude History (Ex. 2)

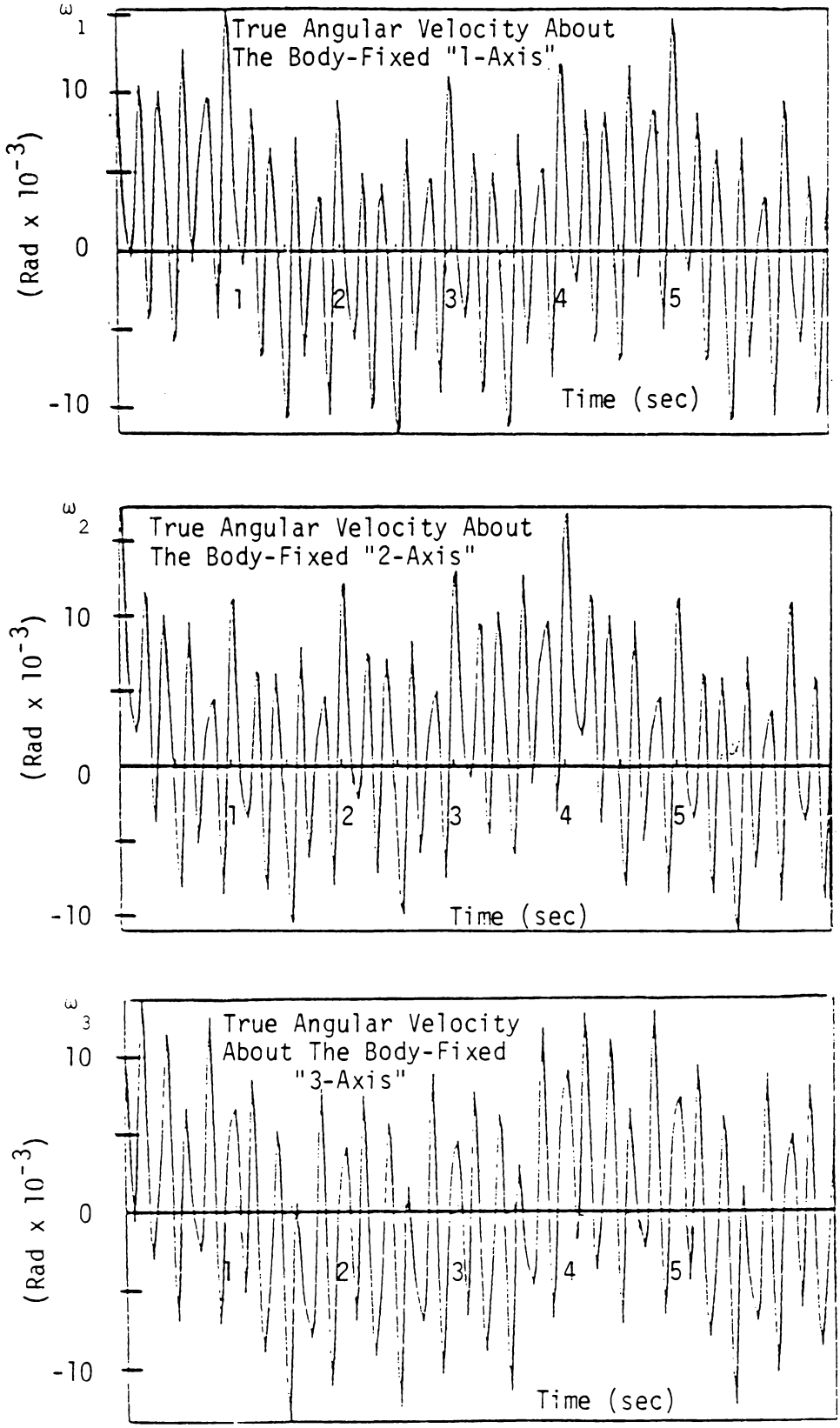

Figure 10 - True Angular Velocity History (Ex. 2)

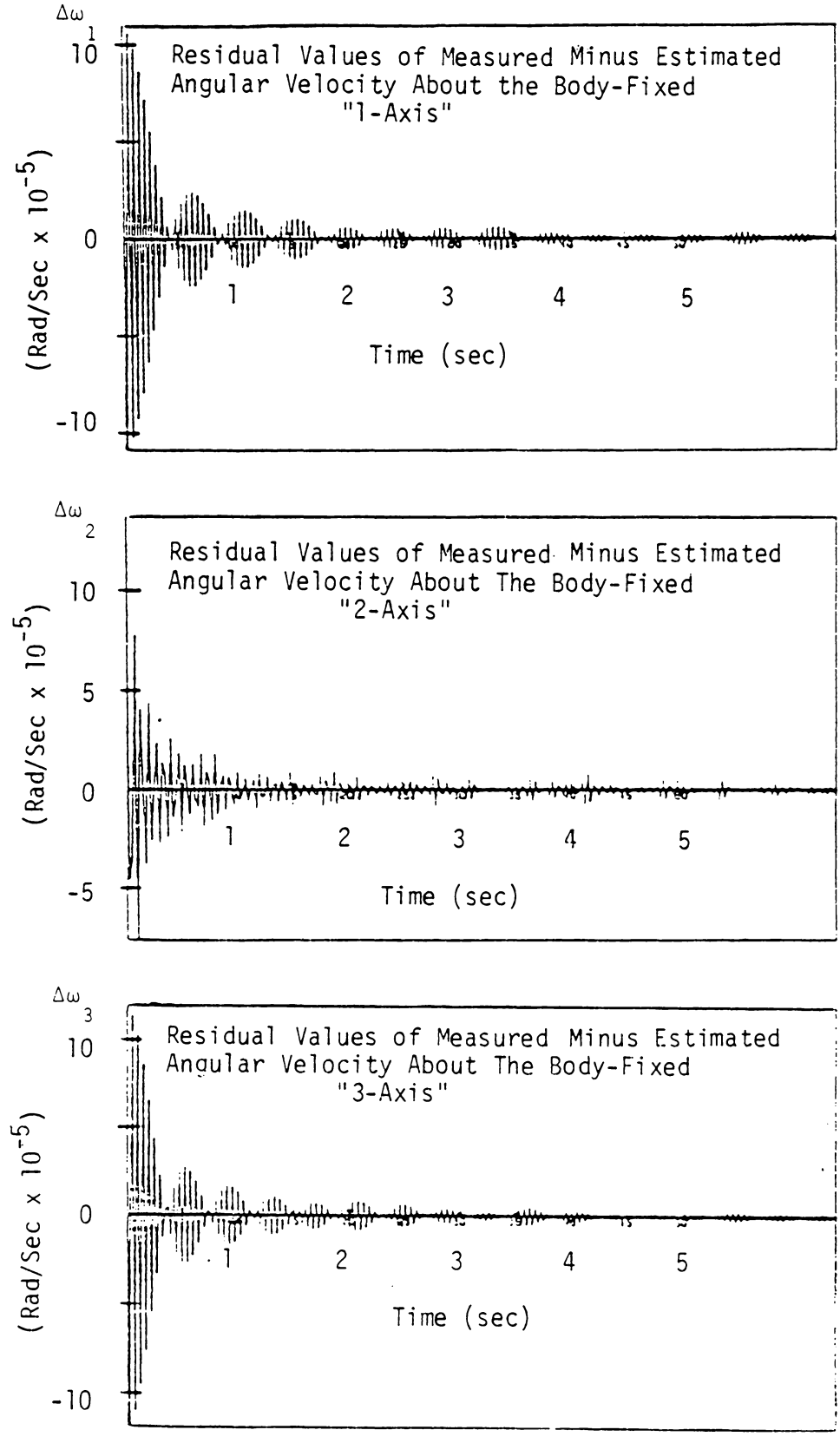

Figure 11 - Measured Minus Estimated Angular Velocity Residuals (Ex. 2)

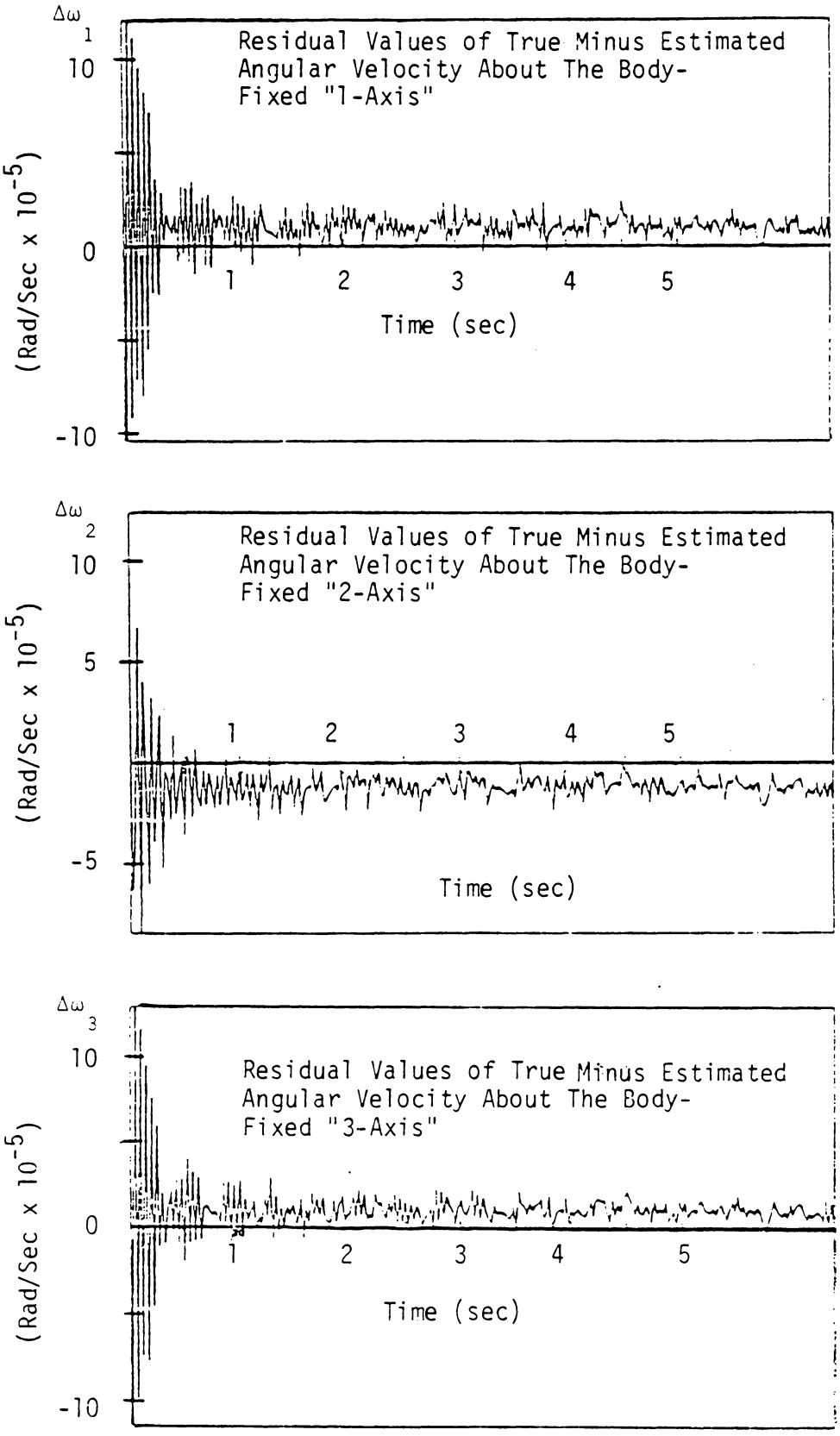

Figure 12 - True Minus Estimated Angular Velocity Residuals (Ex. 2)

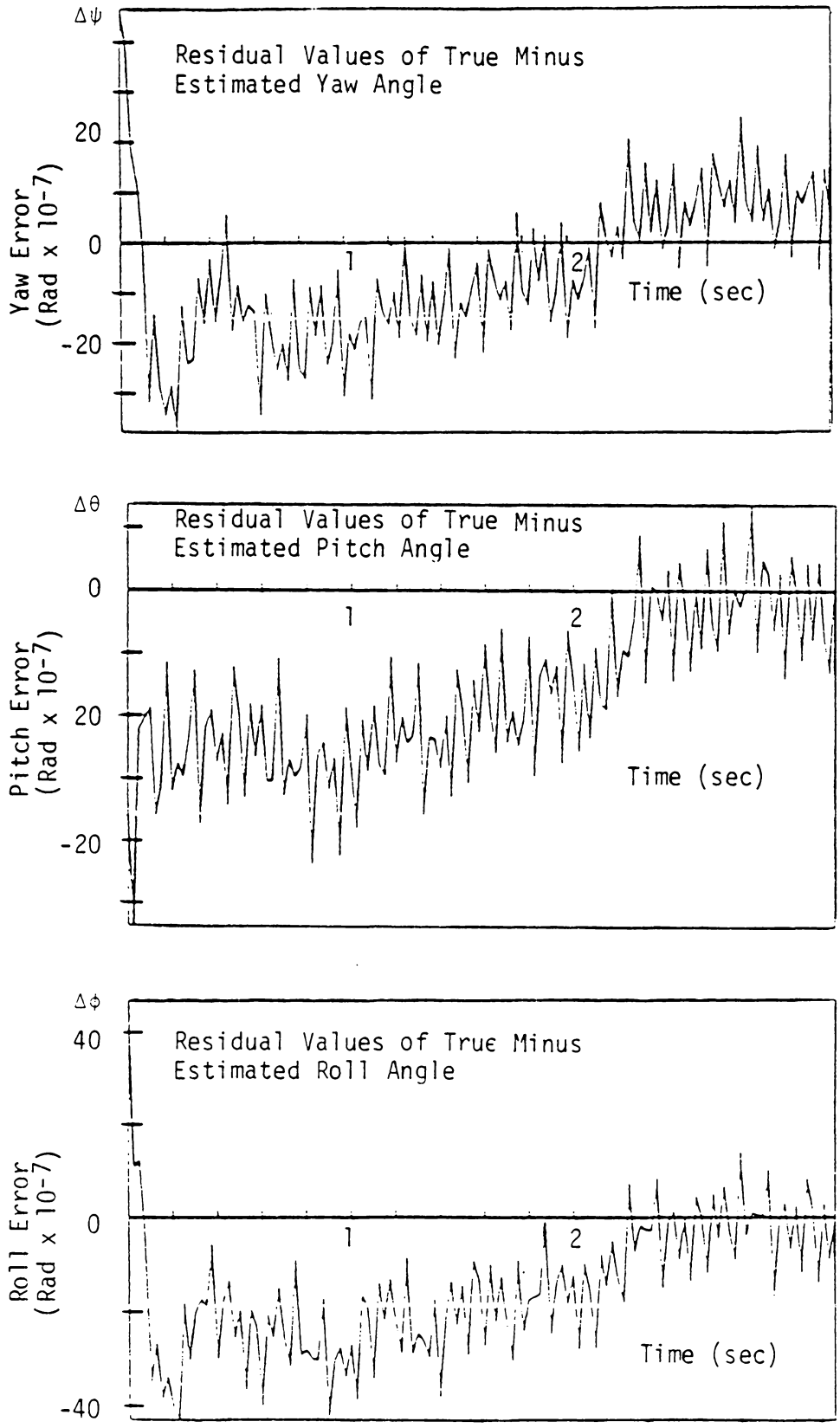

Figure 13 - True Minus Estimated Attitude Residuals (Ex. 2)

5.3 Example 3 - High Noise Motion: Example 3 uses the same frequencies as those found in Example 2 (high and low contributions combined). The same biases were also added to the angular velocity data. In this case, however, the noise superimposed on the angular velocity signal had zero mean and a standard deviation of 5.0×10^{-5} radians/second. This large error is not representative of modern rate sensing devices and is only included here to show the robustness of the algorithm with respect to an unexpectedly large random noise sample. Figs. 14, 15, 16, 17, and 18 relate to this example. Note that the residual quantities in Fig. 16 are somewhat more random than previously encountered because the measurement noise is more dominant than the "beat phenomena" of previous examples. Qualitatively, this type of behavior in the residual plots is more expected and "comfortable" than the periodic nature of the corresponding plots in Examples 1 and 2. It is apparent from this example that the truncation logic does not guarantee that the error due directly to the truncation process is zero, but it does guarantee that it is small. The entries in Table 5 show that although the higher noise is present, acceptable accuracy was still attained by the parameter estimation scheme (the average error in initial attitude is approximately 1.4 arc-sec). It is important to note here that the noise in the star sensor measurements

has the same statistical character as that applied to the stellar measurements in Examples 1 and 2.

Table 5 - Comparison of Results (Ex. 3)

Axis	Quantity	Truth	Estimate
1	I.C.	0.16072×10^{-2}	0.16147×10^{-2}
	Bias	0.10000×10^{-4}	0.11350×10^{-4}
	# Coeff. Reqd.		334
2	I.C.	0.64963×10^{-3}	0.66577×10^{-3}
	Bias	-0.12000×10^{-4}	-0.10705×10^{-4}
	# Coeff. Reqd.		275
3	I.C.	0.43527×10^{-2}	0.43595×10^{-2}
	Bias	0.97000×10^{-5}	0.11148×10^{-4}
	# Coeff. Reqd.		296

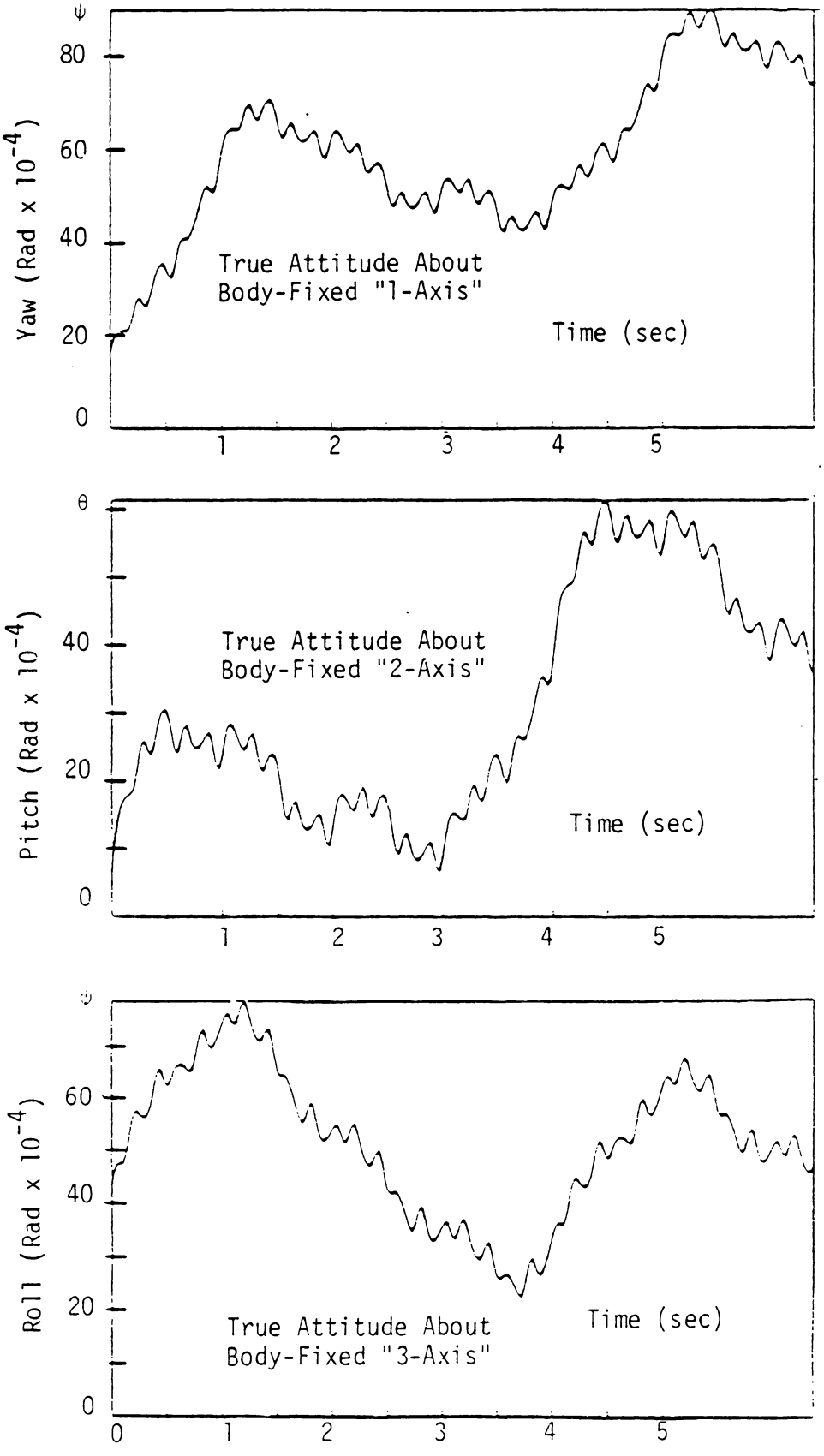

Figure 14 - True Attitude History (Ex. 3)

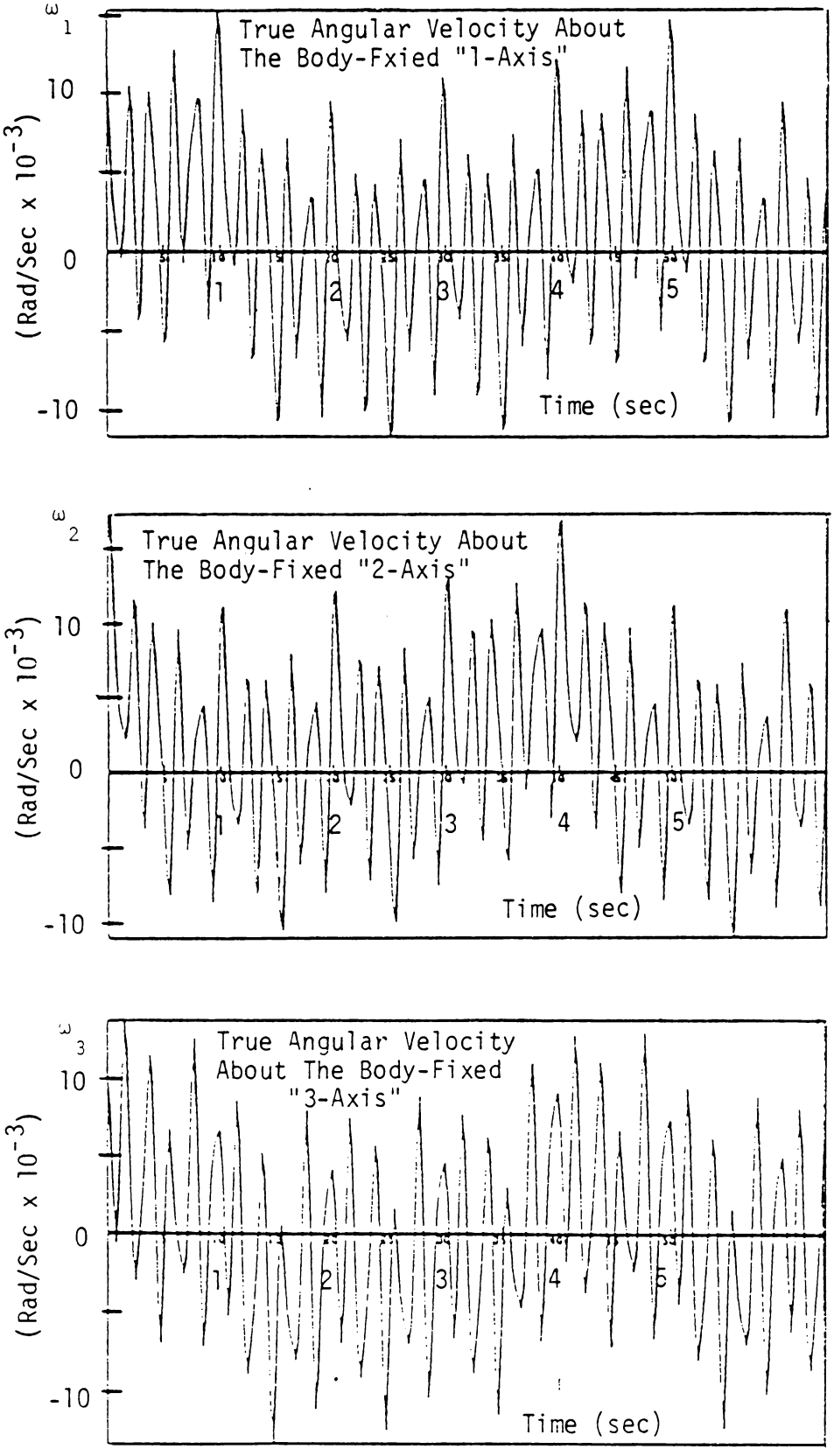

Figure 15 - True Angular Velocity History (Ex. 3)

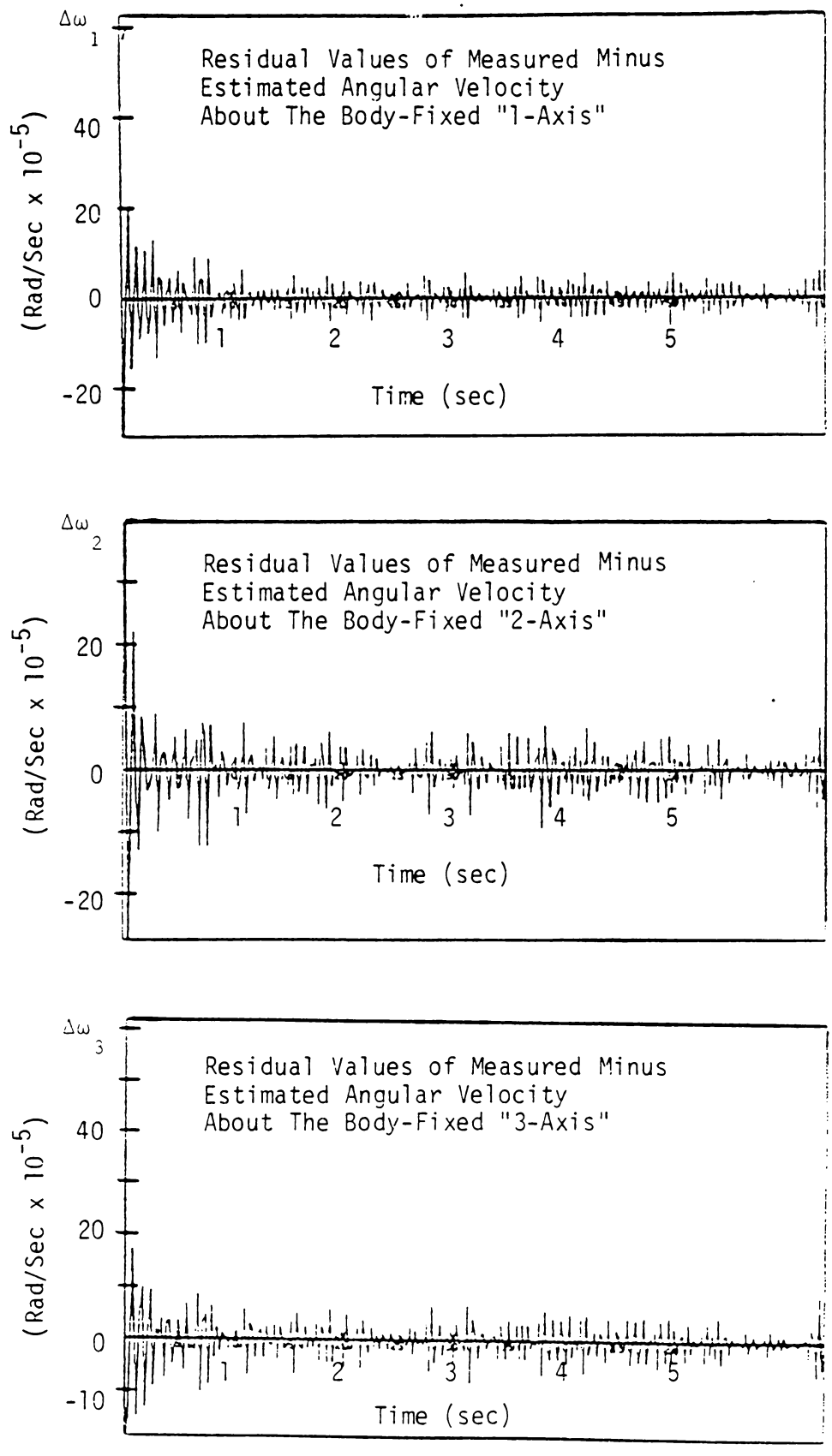

Figure 16 - Measured Minus Estimated Angular Velocity Residuals (Ex. 3)

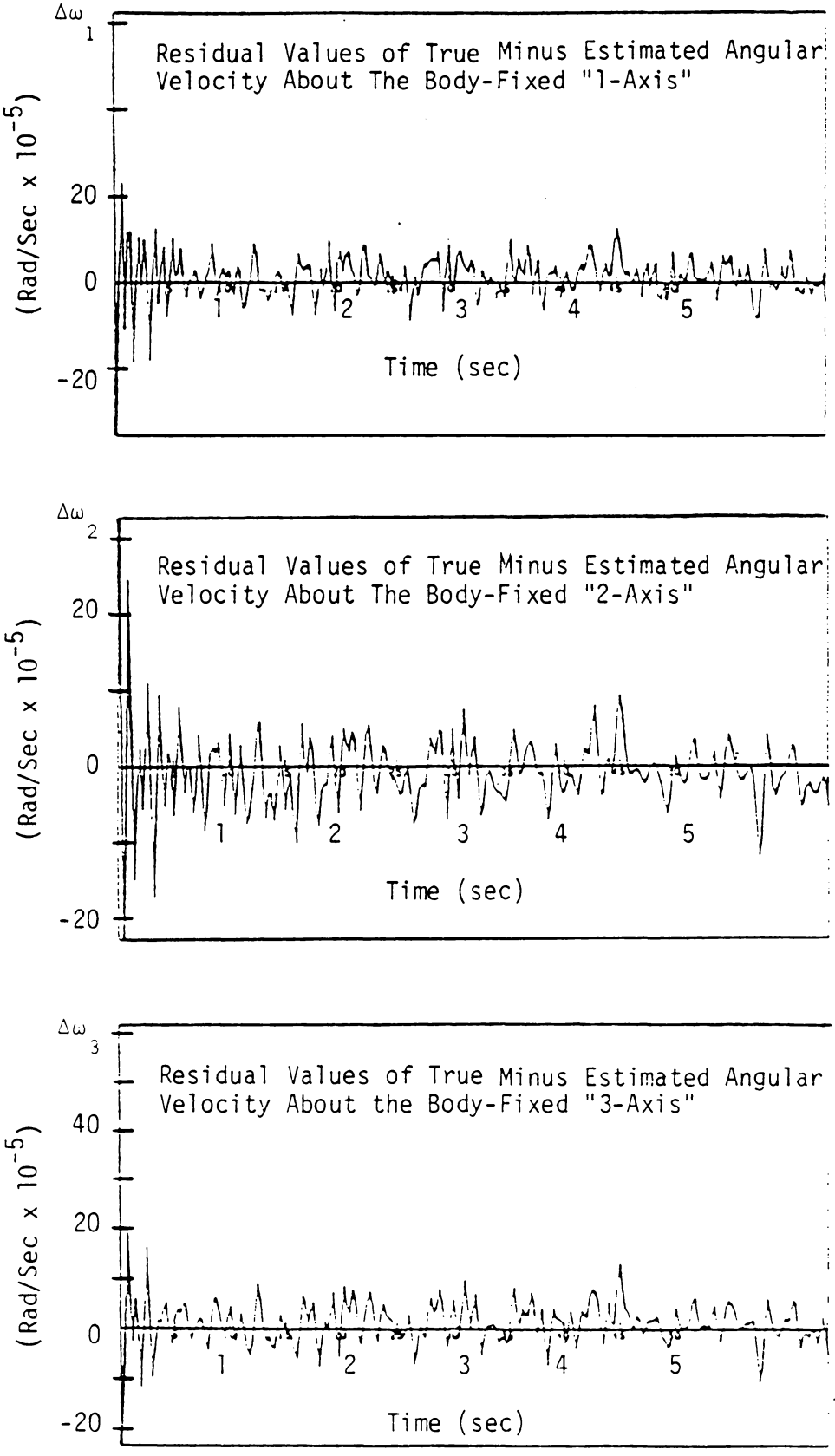

Figure 17 - True Minus Estimated Angular Velocity Residuals (Ex. 3)

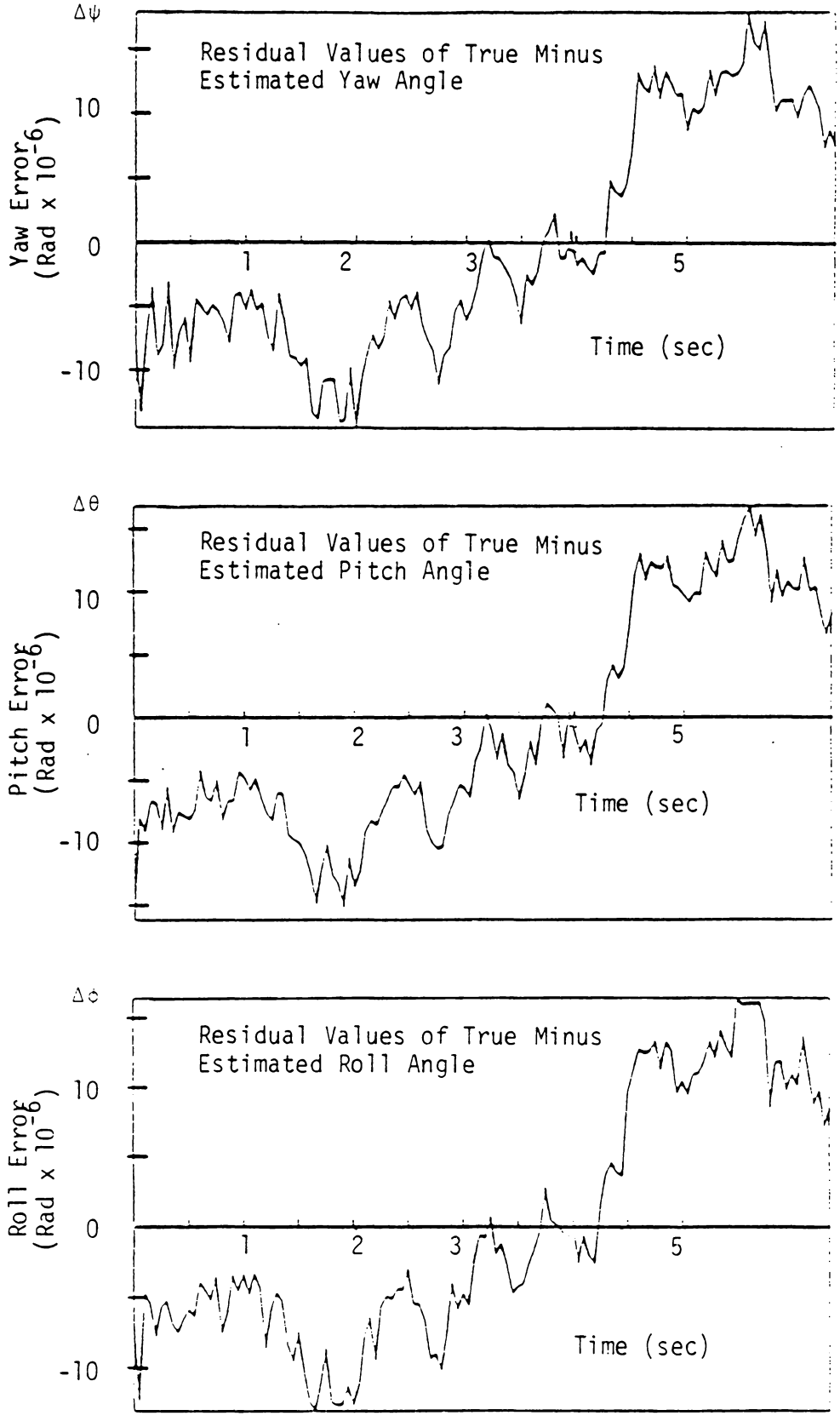

Figure 18 - True Minus Estimated Attitude Residuals (Ex. 3)

5.4 Example 4 - Precision Attitude Determination: In this example, Table 6 shows the frequency content and the respective amplitude of the sine wave that generated the attitude history. There are two differences between this example and Example 2: there is only one frequency contributing to the attitude motion - the lowest frequency in Example 2 - and the largest amplitude to be found in the attitude motion here is 5.84×10^{-4} (an order of magnitude less than the corresponding frequency in the second example). Even though one frequency was used to generate the angular history, several terms are required in the Fourier Series to approximate the angular velocity history since the kinematic equations (Eqs. 2.7) are enforced. The noise added to the angular velocity measurements had zero mean and a standard deviation of 5.0×10^{-6} (equal to the noise in Examples 1 and 2). Table 7 indicates that the initial conditions on the angular displacements have an average error of approximately 0.03 arc-sec.

The figures that correspond to this example are Figs. 19, 20, 21, 22, and 23. In the graphs of the measured minus estimate residuals (Fig. 21), the periodicity is apparently eliminated in this example. This behavior is more consistent with the plot expected from a least squares approximation. When relatively few coefficients are truncated to arrive at an approximation with the residual

statistics desired, the measured minus estimated residuals appear periodic (obvious in the first three examples). In this example, over 80% of the maximum of 500 coefficients were truncated and the residual plots were more typical of those expected from least squares approximation. Note also that the true motion and angular velocity (Figs. 19 and 20) appear almost trivial, but this triviality was necessary to achieve the desired appearance of Fig. 21. (In Fig. 20(b), the angular velocity is nearly constant at 13×10^{-4} rad/sec.)

Table 6 - Frequencies Present in Attitude History (Ex. 4)

Freq. [cps]	Amp. [rad]
0.01667	5.84×10^{-4}

Table 7 - Comparison of Results (Ex. 4)

Axis	Quantity	Truth	Estimate
1	I.C.	0.36768×10^{-3}	0.36774×10^{-3}
	Bias	0.10000×10^{-4}	0.10375×10^{-4}
	# Coeff. Reqd.		91
2	I.C.	-0.39973×10^{-5}	0.37350×10^{-5}
	Bias	-0.12000×10^{-4}	-0.11637×10^{-4}
	# Coeff. Reqd.		94
3	I.C.	0.30601×10^{-3}	0.30625×10^{-3}
	Bias	0.97000×10^{-5}	0.10065×10^{-4}
	# Coeff. Reqd.		94

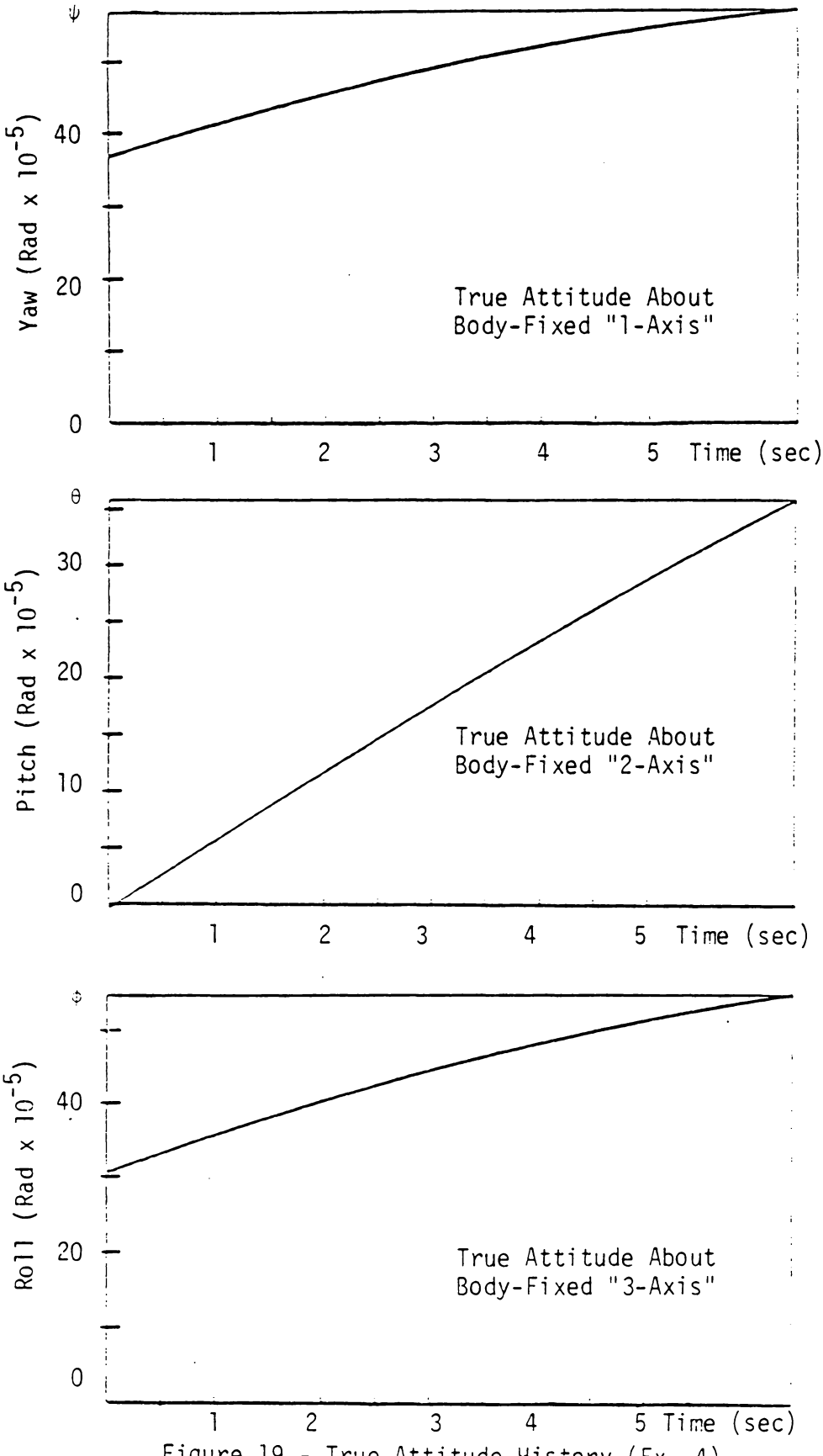

Figure 19 - True Attitude History (Ex. 4)

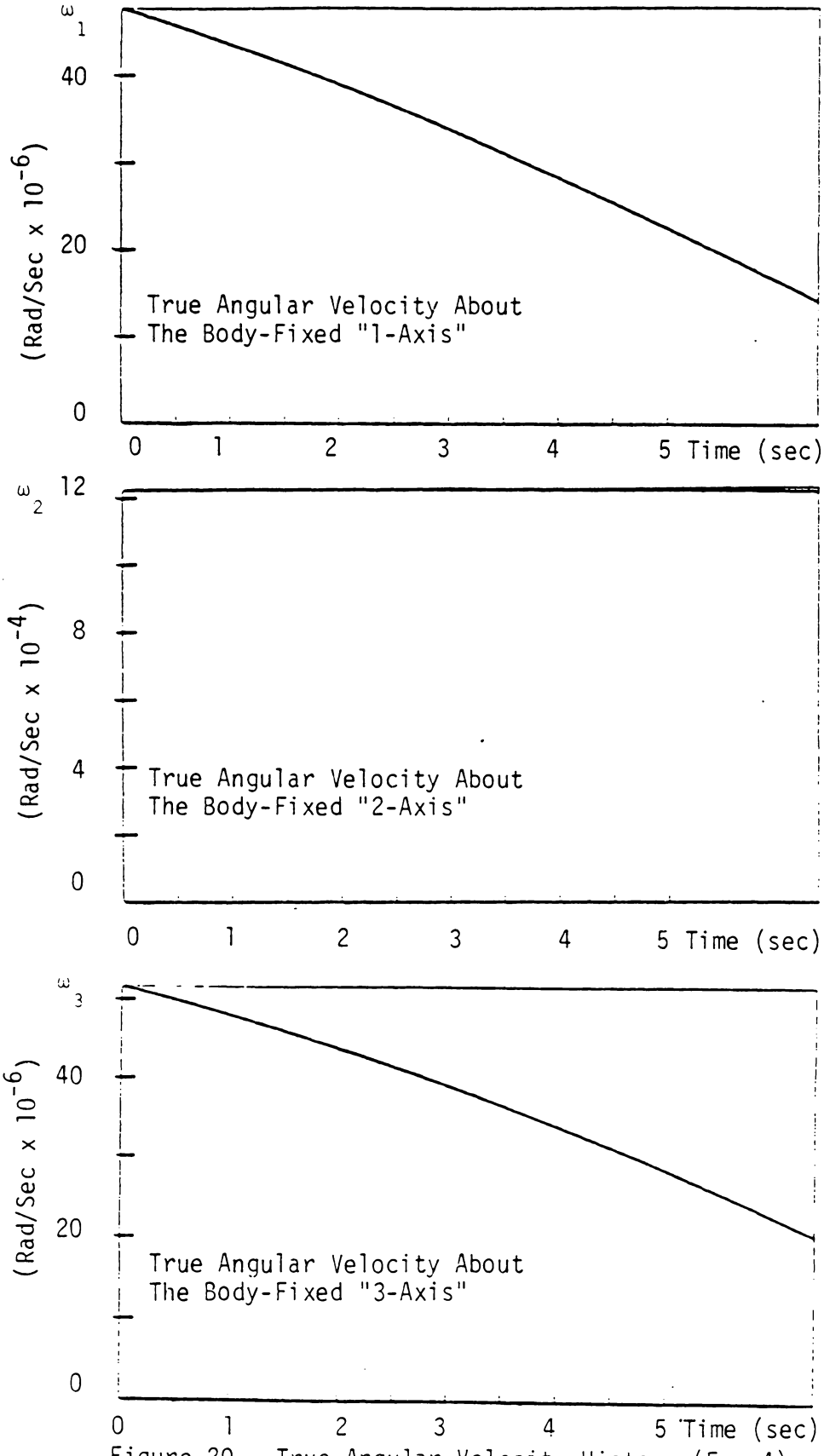

Figure 20 - True Angular Velocity History (Ex. 4)

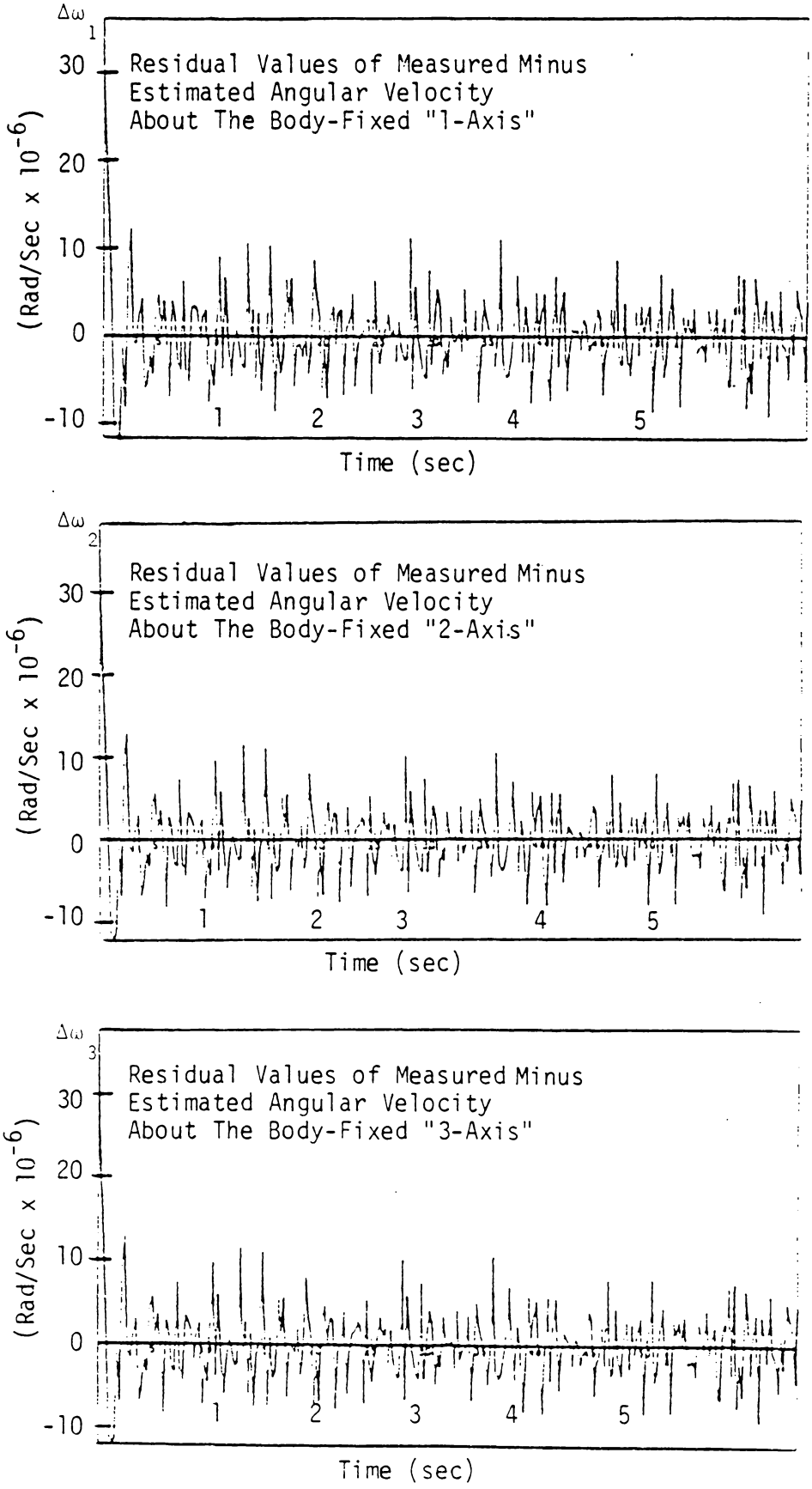

Figure 21 - Measured Minus Estimated Angular Velocity Residuals (Ex. 4)

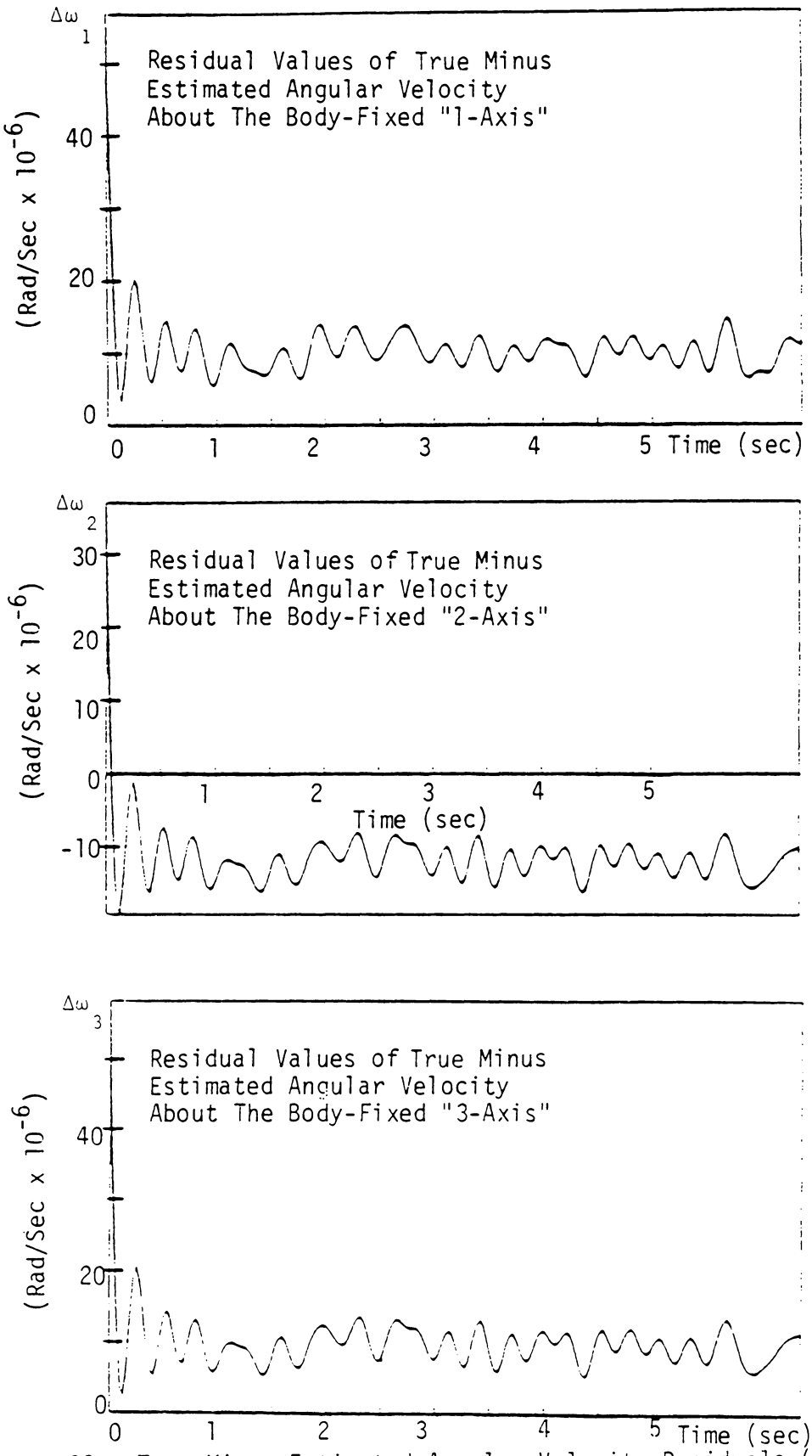

Figure 22 - True Minus Estimated Angular Velocity Residuals (Ex. 4)

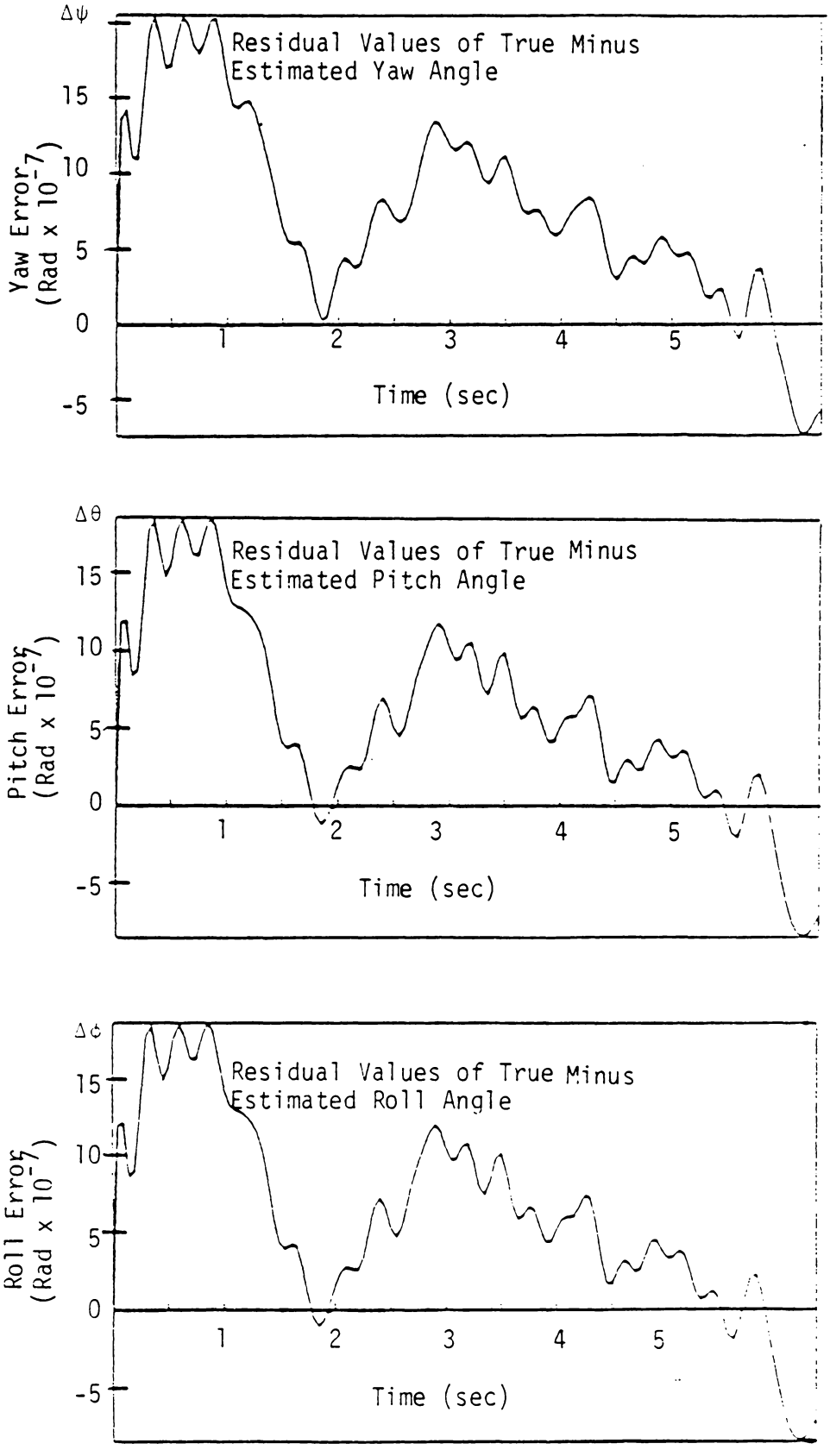

Figure 23 - True Minus Estimated Attitude Residuals (Ex. 4)

CHAPTER 6

CONCLUSIONS AND RECOMMENDATIONS

6.0 Overview: In this chapter, a brief summary of the progress during the research involved in the development of the software presented is given. Several conclusions are drawn based on the numerical examples in Chapter 5 and observations are made concerning the process as a whole. Recommendations are given for further research and areas deserving or requiring future study.

6.1 Research Summary: In the numerical study of Chapter 5, the method presented here is found to be acceptably accurate. An important aspect of the algorithm not discussed until now is the execution time of the smoothing and analysis algorithms: For the 1000 points adjusted in both of the examples presented, the smoothing process has been streamlined to perform its task for the second example in Chapter 5 in slightly more than one minute using an IBM mainframe computer and the FORTRAN computer language. The attitude and bias estimation program is much faster and accomplishes its task in less than 10 seconds under the same circumstances. Previous versions of the attitude and bias estimation algorithm did not recognize convergence in certain instances. The present form of the estimation

routine typically requires only two to three iterations before convergence is reached.

Previous versions of the smoothing algorithm required slightly more than one hour to obtain results comparable with those obtained with the present algorithm. The dramatic improvement in execution time was obtained by various re-structurings of the method used to obtain the Fourier coefficients and efficiently approximate the goodness of fit. This particular facet, together with the number of times that the complete series must be evaluated, proved to be the most time-consuming parts of the program.

6.2 Conclusions and Recommendations: As stated in the last section, the method as a whole has been shown to be acceptably accurate and as such is a success. Other integration schemes are available for use in the estimation routine in the pursuit of greater accuracy and/or less execution time. The Runge-Kutta method used in the program presented here uses a combination of four estimates to determine the slope at a point whereas other methods of integration use a greater number, yielding a more accurate estimate of the integral in question. Other classes of integration methods, namely the predictor-corrector methods, promise more accurate results than the standard four-cycle Runge-Kutta method as well.

There are several phenomena exhibited in the examples of Chapter 5 that are not fully understood and/or could be a source of error for very large volumes of data. These items are left as suggestions for future study: The Gibb's phenomenon, although highly localized at the endpoints of the data admits an uncertainty into the smoothed estimate of angular velocity. This uncertainty does not seem to affect the accuracy of the six parameters recovered, which is in itself puzzling. "Windowing" the data is likely to be a viable solution, but the problem of determining the extent of the influence of the phenomenon in each particular data set remains to be resolved. Intuitively, the residuals of measured minus estimated angular velocity were expected to appear more random, with less periodic structure than was exhibited in the first three examples. Further study of the frequency content of the residual errors is therefore recommended along with the investigation of methods to decrease or eliminate this periodicity while still providing an approximation consistent with the error characteristics of the rate gyroscopes.

In short, the recommendation is made that any further research in this area be concentrated on improving the accuracy and shortening the execution time of the programs presented in this thesis as well as further analyzing the

above truncation/approximation issues so that the approach presented here may be more rigorously applied.

REFERENCES

1. Garg, S. C., Morrow, L. D., and Mamen, R., "Strapdown Navigation Technology: A Literature Survey," Journal of Guidance and Control, Vol. 1, No. 3, May-June 1978, Page 161.

2. Roantree, J. P., "Advancements in Strapdown Navigation," Proceedings of NAECON, May 1974, Page 548.

3. Duffy, T. J., "Concept to Enhance Strapdown Navigation on MaRV's," Journal of Guidance and Control, Vol. 2, No. 6, Page 542.

4. Robinette, G. J., and Schwarz, R. M., "Strapdown Inertial Performance Needed for the 1990's," Transactions of IEEE 1982, Page 364.

5. Motrensen, R. E., "Strapdown Guidance Error Analysis," IEEE Transactions on Aerospace and Electronic Systems, Vol. AES-10, July, 1974, Page 451.

6. Sargent, D,, and Zarett, H., "The Critical Dynamic Errors of a Strapdown Guidance System," Journal of Guidance and Control, Vol. 8, No. 12, Page 1208.

7. Dougherty, H. J., Pelka, E. J., and Rodden, J. J., "Strapdown Attitude Reference Systems: Preliminary Design and Performance Analysis," Journal of Guidance and Control, Vol. 4, No. 4, Page 390.

8. Greenwood, D. T., Principles of Dynamics, Prentice-Hall, Englewood Cliffs, New Jersey, 1965.

9. Grubin, C., "Derivation of the Quaternion Scheme via the Euler Axis and Angle," Journal of Spacecraft and Rockets, Vol. 7, Oct., 1970, Page 1261.

10. Junkins, J. L., Lectures in Analytical Dynamics, unpublished.

11. Mc Aloon, K. J., Farrenkopf, R. L., Belsky, F. J., and Mann, R. J., "Performance Tests of Two Precision Attitude Determination Systems,", Journal of Guidance and Control, Vol. 1, No. 5, Sept.-Oct. 1975, Page 327.

12. Junkins, J. L., An Introduction to Optimal Estimation of Dynamical Systems, Sijthoff and Noordhoff, Leyden, The Netherlands, 1978.

13. Newland, D. E., An Introduction to Random Vibrations and Spectral Analysis, Longman Group Limited, Burnt Mill, Harlow, Essex, U. K., 1975.

14. Bloomfield, P., Fourier Analysis of Time Series: An Introduction, John Wiley and Sons, Inc., New York, New York, 1976.

15. Mikhail, E. M., and Gracie, G., Analysis and Adjustment of Survey Measurements, Van Nostrand Reinhold Company, Inc., New York, New York, 1981.

16. Wolf, P. R., Adjustment Computations, P. B. L. Publishing Co., Monona, Wisconsin, 1980.

17. Gottleib, D. M., "SKYMAP System Description: Star Catalog Database Generation and Utilization", Computer Sciences Corporation Report CSC/SD-76/6041, Nov. 1976, Silver Springs, MD.

18. Kirk, D. E., Optimal Control Theory: An Introduction, Prentice-Hall, Inc., Englewood Cliffs, New Jersey, 1970.

19. Junkins, J. L., Strikwerda, T. E., Kraige, L. G., "Star Pattern Recognition and Spacecraft Attitude Determination", U. S. Army Engineering Topographic Laboratories, Report no. ETL-0173, May, 1981.

20. Raisinghani, S. C. and Bilimoria, K. D., "A New Method for Data Pre-processing", Journal of Guidance and Control, Vol. 7, No. 2, March-April 1984, Page 255.

21. Shanahan, T. G., "System Parameter Refinement for Low-Momentum Reaction Wheel Attitude Control Systems", M. S. Thesis, Virginia Polytechnic Institute and State University, June, 1984.

APPENDIX

PROGRAM LISTINGS

```
C  ***********************************************************************
C  *                      DATA GENERATOR PROGRAM                         *
C  *  THIS PROGRAM GENERATES AN ASSUMED ANGULAR VELOCITY HISTORY         *
C  *  SIMILAR TO SUCH A HISTORY OBTAINED FROM A SATELLITE RATE           *
C  *  GYROSCOPE.  THE HISTORY HAS NINE FREQUENCIES, EACH AT RANDOM       *
C  *  PHASE SHIFTS, AND PRODUCED AS SINUSOIDS.                           *
C  *                                                                     *
C  *                     VARIABLES USED IN PROGRAM                       *
C  *                                                                     *
C  *  AMP(9) - AMPLITUDES OF THE VARIOUS SINUSOIDS,                      *
C  *  F(9) - FREQUENCIES OF THE VARIOUS SINUSOIDS,                       *
C  *  PS(9) - PHASE SHIFTS OF THE VARIOUS SINUSOIDS,                     *
C  *  NB - NUMBER OF ANGULAR VELOCITY DATA POINTS DESIRED (NBP1=         *
C  *       NB+1),                                                        *
C  *  AVAL(I,NBP1) - VALUE OF THE ATTITUDE ANGLE ABOUT THE ITH           *
C  *                 AXIS AT TIME-STEP J,                              *
C  *  BIAS(3) - THE CONSTANT BIAS ASSOCIATED WITH EACH AXIS,             *
C  *  OO - ORBITAL FREQUENCY,                                            *
C  *  TOL - TOLERANCE TO JUSTIFY A "COMPUTER ZERO",                      *
C  *  T - TIME DERIVED FROM THE TIME-STEP SUBSCRIPT,                     *
C  *  TSS - TIME (IN SECONDS) BETWEEN STAR SHOTS,                        *
C  *  ANGT(4) - VALUES OF THE ATTITUDE ANGLES AT TIME T,                 *
C  *  SN(3,3) - TRANSFORMATION MATRIX BETWEEN THE STAR SENSOR TO         *
C  *            THE INERTIAL REFERENCE FRAME,                            *
C  *  ISF - FLAG DENOTING THE RIGHT (ISF=1) OR LEFT STAR SENSOR,         *
C  *  CORT(3) - FIDUCIAL COORDINATES OF THE STAR IMAGE,                  *
C  *  EL(3) - DIRECTION COSINE VECTOR IN THE INERTIAL FRAME TO THE       *
C  *          STAR SENSED,                                               *
C  *  ARAT(I,NB) - VALUE OF THE ANGULAR RATES DEFINED BY KINEMATIC       *
C  *               EQUATIONS FOR THE 1-2-3 EULER ANGLE SEQUENCE,         *
C  *  SS - NO. OF SAMPLES PER SECOND.                                    *
C  ***********************************************************************
      IMPLICIT REAL*8 (A-H,O-Z)
      DOUBLE PRECISION AVAL(3,1203),ARAT(3,1203),A(3,1202),BIAS(3),
     1ANOI(2404)
C  *** SET INITIAL VALUES
C
      SS=40.D+0
      NB=1001
C
      PI=3.141592653589793D+0
      NBP1=NB+1
      VAL=PI/180.D+0
      OO=2.D+0*PI/90.D+0/60.D+0
      NR=0
      BIAS(1)=1.D-05
      BIAS(2)=-1.2D-05
      BIAS(3)=9.7D-06
C  *** PRINT TRUE BIASES TO THE ARCHIVE FILE
      WRITE(8,92)(BIAS(I),I=1,3)
 92   FORMAT(' THE TRUE RATE GYRO BIASES ARE:',/,3D25.16)
C  *** GENERATE DATA SET
```

```
      CALL GEN(PI,NB,NBP1,VAL,OO,AVAL,ARAT,A,NR,SS)
C  *** PRINT THE PURE (NO ERRORS) ANGULAR VELOCITY DATA
      DO 120 I=1,NB
 120     WRITE(12,121)(A(J,I),J=1,3)
 121  FORMAT(3D25.16)
C  *** BIAS THE DATA SET & ADD NOISE (1 SIGMA = 1 DEG/HR)
      DO 93 I=1,NB
 93      ANOI(I)=0.D+0
      CALL GGNML(1984.,4808,ANOI)
      FACT=2.D+0*PI
      DO 95 I=1,3
         DO 95 J=1,NBP1
            T=(J-1)/SS
 95         A(I,J)=A(I,J)-BIAS(I)+ANOI(J)*5.D-06
C  *** PRINT DATA SET
      DO 100 I=1,NB
 100     WRITE(6,110) A(1,I),A(2,I),A(3,I)
 110  FORMAT(3D25.16)
      STOP
      END
      SUBROUTINE GEN(PI,NB,NBP1,VAL,OO,AVAL,ARAT,A,NR,SS)
C
C  GENERATES AN ANGULAR HISTORY WITH THE STATED AMPLITUDE AND FREQUENCY
C  CONTENT.  GENERATES A STAR-HIT AT EACH OF THE REQUIRED TIMES.
C
      IMPLICIT REAL*8 (A-H,O-Z)
      DOUBLE PRECISION AVAL(3,NBP1),ARAT(3,NBP1),A(3,NB),PS(3,20),
     1AMP(9),F(9),ANGT(4),SN(3,3),EL(3),CORT(3),SNT(3,3),PS1(20),
     2PS2(20),PS3(20)
      ONB=1.D+0*NB
      TOL=1.D-08
      ISF=2
C  *** SET AMPLITUDES AND FREQUENCIES USED IN ANGULAR HISTORIES
      DO 3 I=1,9
 3       AMP(I)=0.D+0
      AMP(1)=5.25D-05
      F(1)=8.D+0
      AMP(2)=2.17D-04
      F(2)=5.D+0
      AMP(3)=1.05D-04
      F(3)=3.D+0
      AMP(4)=3.14D-04
      F(4)=1.D+0
      AMP(5)=3.93D-04
      F(5)=5.D-01
      AMP(6)=1.05D-04
      F(6)=25.D-02
      AMP(7)=1.05D-04
      F(7)=2.D-01
      AMP(8)=1.57D-03
      F(8)=1.D+0/12.D+0
      AMP(9)=5.84D-03
```

```
      F(9)=1.D+0/60.D+0
      FA=2.D+0*PI
      DO 12 I=1,20
         PS1(I)=0.D+0
         PS2(I)=0.D+0
 12      PS3(I)=0.D+0
      CALL GGNPM(1.D+0,40,PS1)
      CALL GGNPM(2.D+0,40,PS2)
      CALL GGNPM(3.D+0,40,PS3)
      DO 40 I=1,20
         PS(1,I)=PS1(I)
         PS(2,I)=PS2(I)
 40      PS(3,I)=PS3(I)
C  *** GENERATE ANGULAR AND ANGULAR RATE HISTORIES
      DO 10 I=1,3
         DO 10 J=1,NBP1
            T=(J-1)/SS
            AVAL(I,J)=0.D+0
            ARAT(I,J)=0.D+0
            DO 5 K=1,8
               AVAL(I,J)=AVAL(I,J)+AMP(K)*DSIN(FA*T*F(K)+PS(I,K))
 5          ARAT(I,J)=ARAT(I,J)+F(K)*FA*AMP(K)*DCOS(FA*T*F(K)+PS(I,K))
      AVAL(I,J)=AVAL(I,J)+AMP(9)*DSIN(FA*T*F(9)+PS(I,I+14))
 10   ARAT(I,J)=ARAT(I,J)+F(9)*FA*AMP(9)*DCOS(FA*T*F(9)+PS(I,I+14))
      PER=25.025D+0
      DO 11 J=1,NBP1
         WRITE(9,7) (AVAL(I,J),I=1,3)
 11      WRITE(10,7) (ARAT(I,J),I=1,3)
 7    FORMAT(3D25.16)
C  *** PRINT THE INITIAL VALUES OF ANGLES TO THE ARCHIVE FILE
      WRITE(3,93)AVAL(1,1),AVAL(2,1),AVAL(3,1)
 93   FORMAT(/,' THE TRUE INITIAL ANGLES ARE:',/,3D25.16)
C  ***  CHECK TO SEE IF A STAR SHOT IS NEEDED:  ONCE EVERY TSS SEC
      DO 15 J=1,NBP1
         CALL DECID(J,IFLAG,T,SS)
         IF(IFLAG.EQ.1) GO TO 15
C  ***  LOAD-UP ANGT TO INPUT TO SNCOMP
         ANGT(1)=AVAL(1,J)
         ANGT(2)=AVAL(2,J)
         ANGT(3)=AVAL(3,J)
         ANGT(4)=00*T
C  ***  INCREMENT THE NUMBER OF STAR HITS COUNTER:  NR AND DECIDE ON
C       RIGHT OR LEFT STAR HIT;  ODD# - RIGHT, EVEN # - LEFT
         IF(ISF.EQ.1) THEN
           ISF=2
         ELSE
           ISF=1
         END IF
C  ***  COMPUTE THE TRANSFORMATION MATRIX FROM THE SENSOR TO THE
C       INERTIAL FRAME
         CALL SNCOMP(ANGT,SN,ISF)
C  ***  COMPUTE THE FIDUCIAL COORDINATES OF STAR HIT AND PREPARE SN
```

```
         CALL COORD(SN,CORT,SNT,AK)
C  ***  FIND THE INERTIAL DIRECTION COSINE VECTOR TO THE STAR
         CALL MAMULT(SNT,CORT,EL,3,3,1)
C  ***  ADD NOISE TO MEASURED STAR COORDINATES
         DO 21 I=1,2
 21         CORT(I)=CORT(I)+PS(I,I)*1.D-06/3.D+0
C  ***  PRINT THE COMPONENTS OF THE VECTOR
         WRITE(7,22) T,CORT(1),CORT(2)
 22      FORMAT(3D25.16)
         WRITE(7,23) ISF,EL(1),EL(2),EL(3)
 23      FORMAT(I2,3D25.16)
C        CALL CHECK(SN,EL,AK)
 15   CONTINUE
C  *** FIND THE INERTIAL COMPONENTS WITH A 1-2-3 EULER ANGLE SET
 20   CALL OMEGA(AVAL,ARAT,NB,NBP1,OO,A)
      RETURN
      END
      SUBROUTINE OMEGA(AVAL,ARAT,NB,NBP1,OO,A)
C
C  EVALUATES THE ANGULAR VELOCITY HISTORY BASED ON THE 1-2-3 EULER
C  ANGLE SEQUENCE.
C
      IMPLICIT REAL*8 (A-H,O-Z)
      DOUBLE PRECICION AVAL(3,NBP1),ARAT(3,NBP1),A(3,NBP1)
C  *** CALCULATE THE THREE COMPONENTS OF ANGULAR VELOCITY
      DO 3000 I=1,NB
         A(1,I)=ARAT(1,I)+OO*AVAL(3,I)
         A(2,I)=ARAT(2,I)+OO
 3000    A(3,I)=ARAT(3,I)-OO*AVAL(1,I)
      RETURN
      END
      SUBROUTINE SNCOMP(ANGT,SN,ISF)
C
C  COMPUTES THE TRANSFORMATION MATRIX BETWEEN THE INERTIAL AND STAR-
C  SENSOR FRAME FOR EITHER A RIGHT OR LEFT STAR HIT, DEPENDING ON ISF.
C
      IMPLICIT REAL*8 (A-H,O-Z)
      DOUBLE PRECISION BN(3,3),RB(3,3),LB(3,3),SN(3,3),ANGT(4),DUM(3,3),
     1BO(3,3),D1(3,3),D2(3,3),D3(3,3),ON(3,3)
      CPH=DCOS(ANGT(3))
      CTH=DCOS(ANGT(2))
      CPS=DCOS(ANGT(1))
      SPH=DSIN(ANGT(3))
      STH=DSIN(ANGT(2))
      SPS=DSIN(ANGT(1))
      CG=DCOS(ANGT(4))
      SG=DSIN(ANGT(4))
      F=DSQRT(2.D+0)/2.D+0
      DO 10 I=1,3
         DO 10 J=1,3
            D1(I,J)=0.D+0
            D2(I,J)=0.D+0
```

```
            D3(I,J)=0.D+0
 10         ON(I,J)=0.D+0
      D1(1,1)=1.D+0
      D1(2,2)=CPS
      D1(2,3)=SPS
      D1(3,2)=-SPS
      D1(3,3)=CPS
      D2(1,1)=CTH
      D2(1,3)=-STH
      D2(2,2)=1.D+0
      D2(3,1)=STH
      D2(3,3)=CTH
      D3(1,1)=CPH
      D3(1,2)=SPH
      D3(2,1)=-SPH
      D3(2,2)=CPH
      D3(3,3)=1.D+0
      ON(1,1)=CG
      ON(1,3)=-SG
      ON(2,2)=1.D+0
      ON(3,1)=SG
      ON(3,3)=CG
      CALL MAMULT(D2,D1,DUM,3,3,3)
      CALL MAMULT(D3,DUM,BO,3,3,3)
      CALL MAMULT(BO,ON,BN,3,3,3)
      DO 1000 I=1,3
         DO 1000 J=1,3
            LB(I,J)=0.D+0
 1000       RB(I,J)=0.D+0
      IF (ISF.EQ.1) THEN
         RB(1,1)=1.D+0
         RB(2,2)=F
         RB(2,3)=F
         RB(3,2)=-F
         RB(3,3)=F
         CALL MAMULT(RB,BN,SN,3,3,3)
      ELSE
         LB(1,1)=1.D+0
         LB(2,2)=F
         LB(2,3)=-F
         LB(3,2)=F
         LB(3,3)=F
         CALL MAMULT(LB,BN,SN,3,3,3)
      END IF
      RETURN
      END
      SUBROUTINE MAMULT(T,U,V,L1,L2,L3)
C
C  MULTIPLIES MATRICES T(L1,L2)*U(L2,L3) TO OBTAIN V(L1,L3).
C
      IMPLICIT REAL*8(A-H,O-Z)
      DOUBLE PRECISION T(L1,L2),U(L2,L3),V(L1,L3)
```

```
      DO 1000 I=1,L1
         DO 1000 J=1,L3
            V(I,J)=0.D+0
            DO 1000 K=1,L2
 1000          V(I,J)=V(I,J)+T(I,K)*U(K,J)
      RETURN
      END
      SUBROUTINE COORD(SN,CORT,SNT,AK)
C
C   COMPUTES THE FIDUCIAL COORDINATES OF A STAR HIT AND REVISES SN TO
C   BE MULTIPLIED LATER TO YIELD THE INERTIAL DIRECTION COSINE VECTOR.
C
      IMPLICIT REAL*8 (A-H,O-Z)
      DOUBLE PRECISION SN(3,3),CORT(3),RND(2),SNT(3,3)
      CALL GGNPM(10747.,4,RND)
      CORT(1)=RND(1)*0.005/3.D+0
      CORT(2)=RND(2)*0.005/3.D+0
      CORT(3)=-0.07D+0
      AK=DSQRT(CORT(1)**2+CORT(2)**2+CORT(3)**2)
      DO 10 I=1,3
         DO 10 J=1,3
 10         SNT(I,J)=SN(J,I)/AK
      RETURN
      END
      SUBROUTINE CHECK(SN,EL,AK)
C
C   CHECKS THE DIRECTION COSINE VECTOR PRODUCED BY EVALUATING THE
C   COLLINEARITY EQUATIONS.
C
      IMPLICIT REAL*8 (A-H,O-Z)
      DOUBLE PRECISION SN(3,3),EL(3),SNT(3,3),D(3,3),X(3)
      CALL MAMULT(SN,EL,X,3,3,1)
      BK=DSQRT(EL(1)**2+EL(2)**2+EL(3)**2)
      WRITE(11,7)BK
 7    FORMAT(' MAGNITUDE OF EL (UNITY CHECK):',D25.16,/)
      DO 10 I=1,3
         X(I)=X(I)*AK
         DO 10 J=1,3
 10         SNT(I,J)=SN(J,I)
      CALL MAMULT(SN,SNT,D,3,3,3)
      WRITE(11,15)
 15   FORMAT(' IDENTITY MATRIX CHECK:',/)
      DO 20 I=1,3
 20      WRITE(11,25)(D(I,J),J=1,3)
 25   FORMAT(3D25.16)
      WRITE(11,30)(X(I),I=1,3)
 30   FORMAT(' COORDINATES CHECK:',3D16.8,/)
      RETURN
      END
      SUBROUTINE DECID(J,IFLAG,T,SS)
      IMPLICIT REAL*8 (A-H,O-Z)
      IFLAG=0
```

```
      TOL=1.D-08
      T=(J-1)/SS
C  *** TSS= TIME BETWEEN STAR SHOTS
      TSS=2.D+0
      TF=T/TSS
      ITF=TF+TOL
      DIFF=DABS(TF-ITF)
      IF(DIFF.GT.TOL) IFLAG=1
      RETURN
      END
```

```
C  ***********************************************************************
C  *                                                                     *
C  *               FOURIER SERIES SMOOTHING ALGORITHM                    *
C  *                                                                     *
C  *  THIS PROGRAM FITS A TIME SERIES OF NOISY RATE GYROSCOPE DATA       *
C  *  WITH A FOURIER SERIES UNDER THE CONSTRAINT THAT THE VECTOR         *
C  *  MAGNITUDE OF THE COEFFICIENTS OF THE LAST FREQUENCY UTILIZED       *
C  *  IS THE LAST SUCH MAGNITUDE THAT IS GREATER THAN THE VARIANCE       *
C  *  OF THE RATE GYROSCOPE OUTPUT.                                      *
C  *                                                                     *
C  *             ***  VARIABLES USED IN THE PROGRAM  ***                *
C  *                                                                     *
C  *   A(N) - VECTOR WHICH IS ONE COLUMN OF AVEL,                        *
C  *   ACOEF(INUM) - COEFFICIENTS OF THE COSINES IN THE FOURIER          *
C  *                 SERIES,                                             *
C  *   ACOEF0 - THE FIRST TERM IN THE FOURIER SERIES (D.C. OFFSET),      *
C  *   AVEL(3,N) - MATRIX OF NOISY, UNFILTERED RATE GYROSCOPE DATA,      *
C  *   BCOEF(INUM) - COEFFICIENTS OF THE SINES IN THE FOURIER SERIES,    *
C  *   GVAR - RATE GYROSCOPE VARIANCE SUPPLIED BY THE MFR.,              *
C  *   H - INTERVAL BETWEEN SAMPLES OF THE DATA,                         *
C  *   PER - THE LENGTH OF THE TIME INTERVAL TO BE SMOOTHED,             *
C  *   SS - NUMBER OF SAMPLES OF DATA PER SECOND,                        *
C  ***********************************************************************
      IMPLICIT REAL*8 (A-H,O-Z)
      DOUBLE PRECISION AVEL(3,1201),A(1201),ACOEF(1201),
     1BCOEF(1201),X(1201)
C  *** SET INITIAL VALUES
C
      SS=4.D+1
      N=1001
C
      PI=3.141592653589793D+0
      NM1=N-1
      NM1D2=NM1/2
      NQ=NM1D2+1
      H=1.D+0/SS
      PER=N/SS
C  *** ENTER GYRO STD. DEV. (3 SIGMA) IN RAD/SEC
C
      GSD=5.D-06
C
      GVAR=GSD**2
      WRITE(9,9) GVAR,N
 9    FORMAT(' THE INPUT GYRO VAR.=',D25.16,' (RAD./SEC.)**2',/,' THE
     1TOTAL  NUMBER OF DATA POINTS TO BE FIT=',I5,///)
C  *** READ-IN DATA SET
      DO 12 I=1,N
 12      READ(5,13)(AVEL(J,I),J=1,3)
 13      FORMAT(3D25.16)
C
      DO 96 K=1,3
C
```

```
      DO 15 I=1,N
 15      A(I)=AVEL(K,I)
C  *** EVALUATE THE COEFFICIENTS FOR A PERFECT FIT BY FOURIER SERIES
      DO 20 I=1,NQ
         INUM=I-1
 20      CALL COEFF(PI,N,INUM,H,PER,A,ACOEF0,ACOEF,BCOEF)
      DO 21 I=1,NM1D2
 21      WRITE(10,22)ACOEF(I),BCOEF(I)
 22   FORMAT(2D25.16)
C  ***  COMPUTE THE VARIANCE OF THE RESIDUALS AND SET INUM ACCORDING
C       TO WHERE THE COMPUTED VARIANCE EXCEEDS THE GYRO VARIANCE
      S=0.D+0
      DO 30 I=1,NM1D2
         J=NM1D2-I+1
         S=S+(ACOEF(J)**2+BCOEF(J)**2)/N
         IF(S.GE.GVAR) THEN
            INUM=J
            GO TO 40
         END IF
 30   CONTINUE
C  ***  EVALUATE THE FINAL FIT
      INUM=1
 40   CALL EVAL(PI,PER,N,INUM,H,ACOEF0,ACOEF,BCOEF,X)
C  ***  COMPUTE THE MEAN RESIDUAL AND THE RESIDUAL VARIANCE OVER THE
C       ENTIRE CURVE AS A CHECK
 45   CALL STAT(GVAR,A,X,N,IFLAG,RMEAN,RVAR)
      IF(IFLAG.EQ.1) THEN
         INUM=INUM+1
         CALL ADD(N,PI,INUM,X,ACOEF,BCOEF)
         GO TO 45
      END IF
C     DO 49 I=1,INUM
C49      WRITE(9,51)ACOEF(I),BCOEF(I)
C51   FORMAT(2D25.16)
C  *** OUTPUT THE VALUES PERTAINING TO THE FINAL FIT
      WRITE(9,50) K,INUM,RVAR,RMEAN
 50   FORMAT(' ABOUT BODY-FIXED AXIS',I2,',',I5,' COEFFICIENTS WERE NEED
     1ED',/,' TO FIT THE DATA WITH A FINAL RESIDUAL VARIANCE OF',
     2D25.16,/,' AND A MEAN RESIDUAL OF',D25.16,//)
C  *** STORE THE COMPUTED VALUES
      DO 60 I=1,N
 60      AVEL(K,I)=X(I)
C
 96   CONTINUE
C
C  *** PRINT THE COMPUTED VALUES TO THE ATTITUDE ESTIMATION ROUTINE
      DO 70 I=1,N
 70      WRITE(6,80)(AVEL(K,I),K=1,3)
 80   FORMAT(3D25.16)
      STOP
      END
```

```
      SUBROUTINE COEFF(PI,N,INUM,H,PER,A,ACOEF0,ACOEF,BCOEF)
C
C  COMPUTES THE FOURIER SERIES COEFFICIENTS BASED ON THE LEAST-SQUARES
C  DERIVATION FOR THE COEFFICIENT FORMULAS.
C
      IMPLICIT REAL*8 (A-H,O-Z)
      DOUBLE PRECISION A(N),ACOEF(N),BCOEF(N),CTJ(1201),STJ(1201),
     1CNEXT(1201),SNEXT(1201),CH(1201),SH(1201)
      ANUM=0.D+0
      FAC=2.D+0*PI/PER
      IF(INUM.EQ.0) THEN
         CNEXT(1)=1.D+0
         SNEXT(1)=0.D+0
C  *** SET INITIAL VALUES FOR THE ROUTINE
         DO 10 I=1,N
            ARG=FAC*H*I
            CH(I)=DCOS(ARG)
            SH(I)=DSIN(ARG)
 10         ANUM=ANUM+A(I)
         ACOEF0=ANUM/N
      ELSE
         NM1=N-1
         ZTOL=1.D-08
         ADEN=0.D+0
         BNUM=0.D+0
         BDEN=0.D+0
C  *** IF INUM IS A MULTIPLE OF 100, COMPUTE CNEXT AND SNEXT USING
C      THE STANDARD FORTRAN LIBRARY FUNCTIONS
         FN=INUM/1.D+2
         IFN=FN
         DIF=DABS(FN-IFN)
         IF(DIF.LT.ZTOL) THEN
           NP1=N+1
           DO 40 I=1,NP1
C  *** PLACE ARGUMENT OF TRIG FUNCTIONS LESS THAN 2*PI
              TPI=2.D+0*PI
              ARG=FAC*H*INUM*(I-1)
 35           IF(ARG.GT.TPI) THEN
                ARG=ARG-TPI
                GO TO 35
              END IF
              CNEXT(I)=DCOS(ARG)
 40           SNEXT(I)=DSIN(ARG)
         ELSE
            DO 20 I=1,NM1
C  *** RECURSION FORMULAS TO OBTAIN THE NEXT COLUMNS OF COSINES AND
C      SINES BY INCREMENTING THE FREQUENCY AT EACH TIME CONSIDERED
              CNEXT(I+1)=CNEXT(I)*CH(INUM)-SNEXT(I)*SH(INUM)
 20           SNEXT(I+1)=CNEXT(I)*SH(INUM)+SNEXT(I)*CH(INUM)
         END IF
C  *** ACCUMULATE THE NUMERATOR AND DENOMINATOR OF COEFF. EXPRESSIONS
         DO 50 I=1,N
```

```
            ANUM=ANUM+A(I)*CNEXT(I)
            ADEN=ADEN+CNEXT(I)**2
            BNUM=BNUM+A(I)*SNEXT(I)
 50         BDEN=BDEN+SNEXT(I)**2
C  *** COMPUTE THE FOURIER SERIES COEFFICIENTS
         ACOEF(INUM)=ANUM/ADEN
         BCOEF(INUM)=BNUM/BDEN
      END IF
      RETURN
      END
      SUBROUTINE EVAL(PI,PER,N,INUM,H,ACOEF0,ACOEF,BCOEF,X)
C
C  EVALUATES THE FOURIER SERIES INDICATED BY THE INPUT COEFFICIENTS
C  YIELDING VALUES OF A SMOOTHED TIME SERIES AT THE GIVEN TIME STEPS.
C
      IMPLICIT REAL*8 (A-H,O-Z)
      DOUBLE PRECISION ACOEF(N),BCOEF(N),X(N)
      FAC=2.D+0*PI/N
      DO 10 I=1,N
         X(I)=ACOEF0
         DO 10 J=1,INUM
 10         X(I)=X(I)+ACOEF(J)*DCOS(FAC*(I-1)*J)+BCOEF(J)*DSIN(FAC*
     1(I-1)*J)
      RETURN
      END
      SUBROUTINE STAT(GVAR,A,X,N,IFLAG,RMEAN,RVAR)
C
C  COMPUTES THE RESIDUALS OF THE INPUT DATA AND SMOOTHED ESTIMATE, THE
C  MEAN AND VARIANCE THEREOF AND COMPARES IT TO THE MFRS. SUGGESTED
C  RATE GYROSCOPE VARIANCE.
C
      IMPLICIT REAL*8 (A-H,O-Z)
      DOUBLE PRECISION A(N),X(N),R(1201)
      IFLAG=1
      MF25=(N-1)/4
      ML25=N-MF25
C     NEFF=ML25-MF25
      NEFF=N
      RMEAN=0.D+0
      RVAR=0.D+0
C  *** COMPUTE THE RESIDUALS AT EACH POINT AND THE MEAN OVER THE CURVE
C  *** IF THE SECOND "DO" IS USED IN THE TWO LOOPS FOLLOWING, THE RESID-
C      UALS ARE ONLY COMPUTED AND STATISTICS ONLY VALID FOR THE MIDDLE
C      50% OF THE FIT.
      DO 10 I=1,N
C     DO 10 I=MF25,ML25
         R(I)=A(I)-X(I)
 10      RMEAN=RMEAN+R(I)/NEFF
C  *** COMPUTE THE VARIANCE OF THE RESIDUALS
      DO 20 I=1,N
C     DO 20 I=MF25,ML25
```

```
 20       RVAR=RVAR+(R(I)-RMEAN)**2/(NEFF-1)
C  *** COMPARE THE RESIDUAL VARIANCE TO THE GYRO VARIANCE
       IF(RVAR.LE.GVAR) IFLAG=0
C      WRITE(9,21)RVAR
C21    FORMAT(D25.16)
       RETURN
       END
       SUBROUTINE ADD(N,PI,INUM,X,ACOEF,BCOEF)
C
C  THIS SUBROUTINE ADDS ONE TERM TO THE FOURIER SERIES TO BE CONSIDERED
C
       IMPLICIT REAL*8 (A-H,O-Z)
       DOUBLE PRECISION X(N),ACOEF(N),BCOEF(N)
       FAC=2.D+0*PI/N
       DO 10 I=1,N
          ARG=FAC*(I-1)*INUM
 10       X(I)=X(I)+ACOEF(INUM)*DCOS(ARG)+BCOEF(INUM)*DSIN(ARG)
       RETURN
       END
```

```
C*************************************************************************************
C      PROGRAM TO ADJUST ANGULAR VELOCITY AND STAR-HIT HISTORY TO
C            OBTAIN ANGULAR HISTORY AND RATE GYRO BIASES.
C
C                    *** VARIABLES USED IN PROGRAM ***
C
C  ANGT(I) - IN THE ORDER OF SUBSCRIPTS:  PSI(T), THETA(T), PHI(T)
C            AND GAMMA(T),
C  AVAL(I,J) - ANGULAR VALUE ABOUT AXIS I AT TIME-STEP J,
C  B(I) - RATE GYRO BIAS ABOUT THE ITH AXIS,
C  BLS(I,J) - COEFFICIENT MATRIX FOR THE NORMAL EQUATIONS IN THE
C             GAUSSIAN LEAST SQUARES DIFFERENTIAL CORRECTION
C             (G.L.S.D.C.) ALGORITHM,
C  BLST(I,J) - BLS-MATRIX TRANSPOSED,
C  BN(3,3) - COORDINATE TRANSFORMATION MATRIX BETWEEN THE INERTIAL AND
C            BODY AXES,
C  DC(I) - DIFFERENCE BETWEEN THE MEASURED AND COMPUTED FIDUCIAL
C          COORDINATES,
C  DT - ACTUAL TIME DIFFERENCE (IN SECONDS) BETWEEN SUBSCRIPTED
C       TIME STEPS,
C  DX(I) - DIFFERENTIAL CORRECTIONS TO THE I.C. AND BIAS ESTIMATES,
C  IFC - FLAG INDICATING COMPLETION OF ITERATIONS:
C         =0 - ITERATION CONTINUES
C         =1 - CONVERGENCE COMPLETE TO REQUIRED TOLERANCE,
C  INP - FLAG FOR INPUT MODE:  =0 - NOT READING DATA (ITERATION MODE)
C                              =1 - READING DATA,
C  ISF - FLAG FOR SENSOR DATA:  =1 - READING RIGHT STAR SENSOR
C                               =2 - READING LEFT STAR SENSOR,
C  L(I,J) - MATRIX OF INERTIAL DIRECTION COSINE VECTORS FOR THE ITH
C           STAR-HIT REGISTERED,
C  NSS - NUMBER OF STAR-HITS IN BATCH TO BE ADJUSTED,
C  A(I,J) - MEASURED ANGULAR VELOCITY ABOUT THE ITH AXIS AT THE JTH
C            TIME STEP,
C  OO - ANGULAR VELOCITY OF ORBIT,
C  P(I,J) - PARTIAL OF FIDUCIAL COORDINATE W.R.T. EACH PARAMETER BEING
C           ESTIMATED,
C  PMPH(I,J) - PARTIAL OF THE SN-MATRIX W.R.T. PHI(T),
C  PMPS(I,J) - PARTIAL OF THE SN-MATRIX W.R.T. PSI(T),
C  PMTH(I,J) - PARTIAL OF THE SN-MATRIX W.R.T. THETA(T),
C  SN(3,3) - COORDINATE TRANSFORMATION MATRIX BETWEEN THE INERTIAL
C            AND STAR SENSOR AXES,
C  SS - NO. OF SAMPLES PER SECOND,
C  TIM(I) - TIME OF THE ITH STAR-HIT,
C  TIME(I) - CORRELATION OF THE ITH TIME STEP WITH ACTUAL ELAPSED TIME,
C  TOL - VALUE OF THE LARGEST DIFFERENTIAL CORRECTION ALLOWING
C        TRUNCATION TO BE TERMINATED.
C*************************************************************************************
      IMPLICIT REAL*8(A-H,O-Z)
      DOUBLE PRECISION AVAL(3,601),AEST(3,601),XX(3),DX(6),TIME(601),
     1ANGT(4),LB(3,3),RB(3,3),BN(3,3),SN(3,3),TM(6,6),BLST(6,32),DXP(6),
     2UM(6,6),VM(6,6),PMPS(3,3),PMTH(3,3),PMPH(3,3),EL(3,16),ISF(16),
     3DC(32),P(2,6),B(3),TIM(16),A(3,1200),LP(6),LQ(6,2),R(6),
```

```
     4XM(16),YM(16)
C  *** SET INITIAL VALUES
C
      DOUBLE PRECISION BLS(26,6)
      SS=40.D+0
      NSS=13
      NB=1000
C
      DT=2.D+0/SS
      PI=3.141592653589793D+0
      OO=2.D+0*PI/9.D+1/6.D+1
      FL=0.07D+0
      INP=1
      NQT=NB/2+1
      NQTM1=NQT-1
      TOL=1.D-14
C  *** INITIALIZE ITERATION PARAMETERS
      DO 10 I=1,3
         DXP(I+3)=1.D+06
         DX(I)=0.D+0
         DX(I+3)=0.D+0
         B(I)=0.D+0
 10      AVAL(I,1)=0.D+0
C  *** READ DIRTY DATA FROM FT3D ROUTINE OUTPUT
      DO 15 J=1,NB
 15      READ(4,17) (A(I,J),I=1,3)
 17   FORMAT(3D25.16)
C  *** START ITERATION LOOP
C  *** SET INTEGRATION PARAMETERS
 20   DXPS=0.D+0
      DXS=0.D+0
      T=0.D+0
      TIME(1)=T
C  *** SET-UP CALLING LOOP FOR SUBROUTINE RUNGE
      DO 37 J=1,3
 37      XX(J)=AVAL(J,1)
      DO 40 I=2,NQT
         CALL RUNGE(T,DT,3,XX,A,OO,NB,B)
         IF(I.EQ.NQTM1) DT=NB/SS-T
         TIME(I)=T
         DO 40 J=1,3
 40         AVAL(J,I)=XX(J)
      DO 100 I=1,NSS
         I2=2*I
         I2M=2*I-1
C   ISF=1:  STAR ON RIGHT SENSOR, ISF=2:  STAR ON LEFT SENSOR
         IF(INP.EQ.1) THEN
            READ(5,90) TIM(I),XM(I),YM(I)
            READ(5,95) ISF(I),EL(1,I),EL(2,I),EL(3,I)
         END IF
 90      FORMAT(3D25.16)
```

```
 95       FORMAT(I2,3D25.16)
C  *** INTERPOLATE THE VALUES OF ANGLES AT TIME OF OBSERVATION
          CALL INTERP(AVAL,ANGT,TIM,TIME,NQT,B,OO,I,NSS)
C  *** COMPUTE MATRIX-SN FROM ABOVE ANGLES
          CALL SNCOMP(ANGT,SN,ISF(I))
C  *** COMPUTE XN AND YN
          CALL COORD(SN,XM(I),YM(I),EL,I,NSS,DCX,DCY,DEN,FL)
          DC(I2M)=DCX
          DC(I2)=DCY
C  *** COMPUTE PARTIAL DERIVATIVES
          CALL PARSHL(SN,DEN,ANGT,ISF(I),P,FL,I,NSS,EL,OO)
          DO 100 J=1,6
             BLST(J,I2M)=P(1,J)
 100         BLST(J,I2)=P(2,J)
C  *** EXIT INPUT MODE
       INP=0
C  *** OBTAIN THE ADJ. TO PARAMETER ESTIMATES V.I.A. G.L.S.D.C.
       CALL GLSDC(BLS,BLST,I2,DC,DX)
C  *** CHECK THE MAGNITUDE OF THE DIFFERENTIAL CORRECTIONS
       DO 110 I=4,6
          DXPS=DXPS+DXP(I)**2
 110      DXS=DXS+DX(I)**2
       IF(DXPS.GE.DXS) THEN
          DO 130 J=1,3
C  *** PLACE ATTITUDE ESTIMATE IN STORAGE
             DO 120 I=1,NQT
 120            AEST(J,I)=AVAL(J,I)
C  *** ADD CORR. TO PRESENT ESTIMATES, REPLACE DXP WITH DX, ITERATE
             B(J)=B(J)+DX(J+3)
             DXP(J+3)=DX(J+3)
             AVAL(J,1)=AVAL(J,1)+DX(J)
 130         WRITE(6,131)AVAL(J,1),B(J)
 131      FORMAT(' AVAL=',D16.8,' BIAS=',D16.8)
          WRITE(6,132)
 132      FORMAT(/)
          GO TO 20
       ELSE
C  *** PRINT THE RESULTS OF THE ADJUSTMENT AND THE FINAL ATTITUDE EST.
 500      WRITE(6,600)(AVAL(I,1),I=1,3),(B(I),I=1,3)
 600      FORMAT(' INITIAL CONDITIONS ON THE ANGULAR DISPLACEMENTS:',/,
     13D25.16,/,' ESTIMATED RATE GYRO BIASES:',/,3D25.16)
       DO 610 J=1,NQT
 610      WRITE(7,620)(AEST(I,J),I=1,3)
 620   FORMAT(3D25.16)
       END IF
       STOP
       END
       SUBROUTINE RUNGE(T,DT,NEQ,XX,A,OO,NB,B)
C
C  INTEGRATES THE KINEMATIC EQUATIONS BY 4TH ORDER RUNGE-KUTTA ALGORITHM
C
       IMPLICIT REAL*8 (A-H,O-Z)
```

```
      DOUBLE PRECISION XX(3),YI(3),YJ(3),YK(3),YL(3),
     1UU(3),F(3),A(3,NB),B(3)
      DO 1000 I=1,NEQ
 1000    UU(I)=XX(I)
      CALL FLN(OO,A,XX,F,NB,T,B,DT)
      DO 1010 I=1,NEQ
         YI(I)=F(I)*DT
 1010    XX(I)=UU(I)+YI(I)/2.
      T=T+DT/2.
      CALL FLN(OO,A,XX,F,NB,T,B,DT)
      DO 1020 I=1,NEQ
         YJ(I)=F(I)*DT
 1020    XX(I)=UU(I)+YJ(I)/2.
      CALL FLN(OO,A,XX,F,NB,T,B,DT)
      DO 1030 I=1,NEQ
         YK(I)=F(I)*DT
 1030    XX(I)=UU(I)+YK(I)
      T=T+DT/2.
      CALL FLN(OO,A,XX,F,NB,T,B,DT)
      DO 1040 I=1,NEQ
         YL(I)=F(I)*DT
 1040    XX(I)=UU(I)+(YI(I)+2.*YJ(I)+2.*YK(I)+YL(I))/6.
      RETURN
      END
      SUBROUTINE FLN(OO,A,XX,F,NB,T,B,DT)
C
C  EVALUATES THE FIRST DERIVATIVE OF THE ANGLES TO BE INTEGRATED BY
C  SUBROUTINE RUNGE.
C
      IMPLICIT REAL*8 (A-H,O-Z)
      DOUBLE PRECISION A(3,NB),B(3),XX(3),F(3)
      NTS=T*2.D+0/DT+1
      F(1)=A(1,NTS)+B(1)-OO*XX(3)
      F(2)=A(2,NTS)+B(2)-OO
      F(3)=A(3,NTS)+B(3)+OO*XX(1)
      RETURN
      END
      SUBROUTINE INTERP(AVAL,ANGT,TIM,TIME,NQT,B,OO,L,NSS)
C
C  INTERPOLATES VALUES FOR ANGT-MATRIX AT THE TIME OF THE STAR-SHOT.
C
      IMPLICIT REAL*8 (A-H,O-Z)
      DOUBLE PRECISION AVAL(3,NQT),TIME(NQT),TIM(NSS),ANGT(4)
      PI=3.141592653589793D+0
      TPI=2.D+0*PI
      DO 2000 I=1,NQT
         IF(TIM(L).GT.TIME(I+1)) GO TO 2000
         NSL=I
         NSU=I+1
         ENTF=(TIM(L)-TIME(NSL))/(TIME(NSU)-TIME(NSL))
         GO TO 2010
 2000    CONTINUE
```

```
 2010 DO 2020 I=1,3
 2020 ANGT(I)=AVAL(I,NSL)+ENTF*(AVAL(I,NSU)-AVAL(I,NSL))
      ANGT(4)=00*TIM(L)
C  *** MAKE ANGT(I) FALL BETWEEN 0 AND 2*PI
      DO 2030 I=1,4
 2025    IF(DABS(ANGT(I)).LT.TPI)GO TO 2030
         IF(ANGT(I).GT.0.D+0) THEN
            ANGT(I)=ANGT(I)-TPI
            GO TO 2025
         ELSE
           ANGT(I)=ANGT(I)+TPI
           GO TO 2025
         END IF
 2030    CONTINUE
      RETURN
      END
      SUBROUTINE SNCOMP(ANGT,SN,ISF)
C
C  COMPUTES THE TRANSFORMATION MATRIX BETWEEN THE INERTIAL AND STAR-
C  SENSOR FRAME FOR EITHER A RIGHT OR LEFT STAR HIT, DEPENDING ON ISF.
C
      IMPLICIT REAL*8 (A-H,O-Z)
      DOUBLE PRECISION BN(3,3),RB(3,3),LB(3,3),SN(3,3),ANGT(4)
      CPH=DCOS(ANGT(3))
      CTH=DCOS(ANGT(2))
      CPS=DCOS(ANGT(1))
      SPH=DSIN(ANGT(3))
      STH=DSIN(ANGT(2))
      SPS=DSIN(ANGT(1))
      CG=DCOS(ANGT(4))
      SG=DSIN(ANGT(4))
      F=DSQRT(2.D+0)/2.D+0
      BN(1,1)=CG*CTH*CPH-SG*CPH*CPS*STH+SG*SPS*SPH
      BN(1,2)=CPH*STH*SPS+SPH*CPS
      BN(1,3)=-SG*CTH*CPH-CG*CPH*CPS*STH+CG*SPS*SPH
      BN(2,1)=SG*CPS*STH*SPH-CG*CTH*SPH+SG*SPS*CPH
      BN(2,2)=CPH*CPS-SPH*SPS*STH
      BN(2,3)=SG*CTH*SPH+CPS*STH*SPH*CG+CG*SPS*CPH
      BN(3,1)=CG*STH+SG*CPS*CTH
      BN(3,2)=-CTH*SPS
      BN(3,3)=CG*CPS*CTH-SG*STH
      DO 3000 I=1,3
         DO 3000 J=1,3
            LB(I,J)=0.D+0
 3000       RB(I,J)=0.D+0
      IF (ISF.EQ.1)THEN
         RB(1,1)=1.D+0
         RB(2,2)=F
         RB(2,3)=F
         RB(3,2)=-F
         RB(3,3)=F
         CALL MAMULT(RB,BN,SN,3,3,3)
```

```
      ELSE
         LB(1,1)=1.D+0
         LB(2,2)=F
         LB(2,3)=-F
         LB(3,2)=F
         LB(3,3)=F
         CALL MAMULT(LB,BN,SN,3,3,3)
      END IF
      RETURN
      END
      SUBROUTINE COORD(SN,XM,YM,EL,K,NSS,DCX,DCY,DEN,F)
C
C  COMPUTES THE DIFFERENCE BETWEEN THE MEASURED AND COMPUTED FIDUCIAL
C  COORDINATES.
C
      IMPLICIT REAL*8(A-H,O-Z)
      DOUBLE PRECISION SN(3,3),EL(3,NSS)
      DEN=0.D+0
      XN=0.D+0
      YN=0.D+0
      DO 4000 I=1,3
 4000    DEN=DEN+SN(3,I)*EL(I,K)
      DO 4010 I=1,3
         XN=XN-F*(SN(1,I)*EL(I,K))/DEN
 4010    YN=YN-F*(SN(2,I)*EL(I,K))/DEN
      DCX=XM-XN
      DCY=YM-YN
      WRITE(6,4011)XN,YN,XM,YM
 4011 FORMAT(' XN & YN =',4D16.8)
      RETURN
      END
      SUBROUTINE PARSHL(SN,DEN,ANGT,ISF,P,F,K,NSS,EL,OO)
C
C  COMPUTES THE PARTIAL DERIVATIVES NECESSARY FOR THE BLS-MATRIX.
C
      IMPLICIT REAL*8(A-H,O-Z)
      DOUBLE PRECISION SN(3,3),EL(3,NSS),P(2,6),ANGT(4),PMPS(3,3),
     1PMTH(3,3),PMPH(3,3),DUM(3,3),LB(3,3),RB(3,3)
      CAPX=0.D+0
      CAPY=0.D+0
      DO 5000 I=1,3
         CAPX=CAPX+SN(1,I)*EL(I,K)
 5000    CAPY=CAPY+SN(2,I)*EL(I,K)
      CPH=DCOS(ANGT(3))
      CTH=DCOS(ANGT(2))
      CPS=DCOS(ANGT(1))
      SPH=DSIN(ANGT(3))
      STH=DSIN(ANGT(2))
      SPS=DSIN(ANGT(1))
      CG=DCOS(ANGT(4))
      SG=DSIN(ANGT(4))
      GAMT=ANGT(4)
```

```
      FAC=DSQRT(2.D+0)/2.D+0
C  *** COMPUTE THE MATRIX OF PARTIALS OF BN W.R.T. PSI
      PMPS(1,1)=SG*CPH*SPS*STH+SG*CPS*SPH
      PMPS(1,2)=CPS*CPH*STH-SPH*SPS
      PMPS(1,3)=CG*CPH*SPS*STH+CG*CPS*SPH
      PMPS(2,1)=-SG*SPS*STH*SPH+SG*CPS*CPH
      PMPS(2,2)=-CPS*STH*SPH-SPS*CPH
      PMPS(2,3)=-SPS*STH*SPH*CG+CG*CPS*CPH
      PMPS(3,1)=-SG*SPS*CTH
      PMPS(3,2)=-CTH*CPS
      PMPS(3,3)=-CG*SPS*CTH
C  *** COMPUTE THE MATRIX OF PARTIALS OF BN W.R.T. THETA
      PMTH(1,1)=-CG*STH*CPH-SG*CPH*CPS*CTH
      PMTH(1,2)=CPH*CTH*SPS
      PMTH(1,3)=SG*STH*CPH-CG*CPH*CPS*CTH
      PMTH(2,1)=CG*STH*SPH+SG*CPS*CTH*SPH
      PMTH(2,2)=-SPH*CTH*SPS
      PMTH(2,3)=CG*CPS*SPH*CTH-SG*STH*SPH
      PMTH(3,1)=CG*CTH-SG*CPS*STH
      PMTH(3,2)=STH*SPS
      PMTH(3,3)=-SG*CTH-CG*CPS*STH
C  *** COMPUTE THE MATRIX OF PARTIALS OF BN W.R.T. PHI
      PMPH(1,1)=SG*SPH*CPS*STH-CG*CTH*SPH+SG*SPS*CPH
      PMPH(1,2)=CPH*CPS-SPH*STH*SPS
      PMPH(1,3)=SG*CTH*SPH+CG*SPH*CPS*STH+CG*SPS*CPH
      PMPH(2,1)=SG*CPS*STH*CPH-CG*CTH*CPH-SG*SPS*SPH
      PMPH(2,2)=-SPS*STH*CPH-SPH*CPS
      PMPH(2,3)=SG*CTH*CPH+CPS*STH*CPH*CG-CG*SPS*SPH
      PMPH(3,1)=0.D+0
      PMPH(3,2)=0.D+0
      PMPH(3,3)=0.D+0
C  *** COMPUTE THE TRANSFORMATION MATRIX RB OR LB BASED ON ISF AND
C       MODIFY THE ABOVE PARTIAL DERIVATIVE MATRICES TO BE THE PARTIAL
C       OF SN W.R.T. THE PREVIOUSLY LISTED PARAMETERS
      DO 3000 I=1,3
         DO 3000 J=1,3
            LB(I,J)=0.D+0
 3000       RB(I,J)=0.D+0
      IF (ISF.EQ.1)THEN
         RB(1,1)=1.D+0
         RB(2,2)=FAC
         RB(2,3)=FAC
         RB(3,2)=-FAC
         RB(3,3)=FAC
         CALL MAMULT(RB,PMPS,DUM,3,3,3)
         CALL DUMP(DUM,PMPS,3,3)
         CALL MAMULT(RB,PMTH,DUM,3,3,3)
         CALL DUMP(DUM,PMTH,3,3)
         CALL MAMULT(RB,PMPH,DUM,3,3,3)
         CALL DUMP(DUM,PMPH,3,3)
      ELSE
         LB(1,1)=1.D+0
```

```
         LB(2,2)=FAC
         LB(2,3)=-FAC
         LB(3,2)=FAC
         LB(3,3)=FAC
         CALL MAMULT(LB,PMPS,DUM,3,3,3)
         CALL DUMP(DUM,PMPS,3,3)
         CALL MAMULT(LB,PMTH,DUM,3,3,3)
         CALL DUMP(DUM,PMTH,3,3)
         CALL MAMULT(LB,PMPH,DUM,3,3,3)
         CALL DUMP(DUM,PMPH,3,3)
      END IF
C  *** INITIALIZE THE PARTIAL DERIVATIVE MATRIX FOR G.L.S.D.C.
      DO 5010 I=1,2
         DO 5010 J=1,6
 5010       P(I,J)=0.D+0
C  *** COMPUTE THE PARTIAL DERIVATIVE MATRIX
      DO 5020 I=1,3
         P(1,1)=P(1,1)-F/DEN*EL(I,K)*(PMPS(1,I)*CG+PMPH(1,I)*SG-CAPX
     1/DEN*(PMPS(3,I)*CG+PMPH(3,I)*SG))
         P(2,1)=P(2,1)-F/DEN*EL(I,K)*(PMPS(2,I)*CG+PMPH(2,I)*SG-CAPY
     1/DEN*(PMPS(3,I)*CG+PMPH(3,I)*SG))
         P(1,2)=P(1,2)-F/DEN*EL(I,K)*(PMTH(1,I)-CAPX/DEN*PMTH(3,I))
         P(2,2)=P(2,2)-F/DEN*EL(I,K)*(PMTH(2,I)-CAPY/DEN*PMTH(3,I))
         P(1,3)=P(1,3)-F/DEN*EL(I,K)*(PMPH(1,I)*CG-PMPS(1,I)*SG-CAPX
     1/DEN*(PMPH(3,I)*CG-PMPS(3,I)*SG))
         P(2,3)=P(2,3)-F/DEN*EL(I,K)*(PMPH(2,I)*CG-PMPS(2,I)*SG-CAPY
     1/DEN*(PMPH(3,I)*CG-PMPS(3,I)*SG))
         P(1,4)=P(1,4)-F/DEN*EL(I,K)*(PMPS(1,I)*SG/OO+PMPH(1,I)*(1-CG)
     1/OO-CAPX/DEN*(PMPS(3,I)*SG/OO+PMPH(3,I)*(1-CG)/OO))
         P(2,4)=P(2,4)-F/DEN*EL(I,K)*(PMPS(2,I)*SG/OO+PMPH(2,I)*(1-CG)
     1/OO-CAPY/DEN*(PMPS(3,I)*SG/OO+PMPH(3,I)*(1-CG)/OO))
         P(1,5)=P(1,5)-F/DEN*EL(I,K)*(PMTH(1,I)*GAMT/OO-CAPX/DEN*
     1PMTH(3,I)*GAMT/OO)
         P(2,5)=P(2,5)-F/DEN*EL(I,K)*(PMTH(2,I)*GAMT/OO-CAPY/DEN*
     1PMTH(3,I)*GAMT/OO)
         P(1,6)=P(1,6)-F/DEN*EL(I,K)*(PMPS(1,I)*(CG-1)/OO+PMPH(1,I)*SG
     1/OO-CAPX/DEN*(PMPS(3,I)*(CG-1)/OO+PMPH(3,I)*SG/OO))
 5020    P(2,6)=P(2,6)-F/DEN*EL(I,K)*(PMPS(2,I)*(CG-1)/OO+PMPH(2,I)*SG
     1/OO-CAPY/DEN*(PMPS(3,I)*(CG-1)/OO+PMPH(3,I)*SG/OO))
      RETURN
      END
      SUBROUTINE GLSDC(BLS,BLST,IDM,DC,DX)
C
C  COMPUTES DIFFERENTIAL CORRECTIONS TO THE INITIAL CONDITIONS OF THE
C  INTEGRATION OF THE KINEMATIC EQUATIONS.
C
      IMPLICIT REAL*8(A-H,O-Z)
      DOUBLE PRECISION BLS(IDM,6),DC(IDM),DX(6),BLST(6,IDM),Q(6,6),
     1LP(6),LQ(6,2),R(6)
      DO 10 J=1,6
         DO 10 K=1,IDM
 10         BLS(K,J)=BLST(J,K)
```

```
      CALL MAMULT(BLST,BLS,Q,6,IDM,6)
      CALL MAMULT(BLST,DC,DX,6,IDM,1)
      CALL GAUSS(Q,DX,6,1,1,LP,LQ,R)
      RETURN
      END
      SUBROUTINE MAMULT(TM,UM,VM,L1,L2,L3)
C
C  MULTIPLIES MATRICES TM(L1,L2)*UM(L2,L3) TO OBTAIN VM(L1,L3).
C
      IMPLICIT REAL*8(A-H,O-Z)
      DOUBLE PRECISION TM(L1,L2),UM(L2,L3),VM(L1,L3)
      DO 7000 I=1,L1
         DO 7000 J=1,L3
            VM(I,J)=0.D+0
            DO 7000 K=1,L2
 7000          VM(I,J)=VM(I,J)+TM(I,K)*UM(K,J)
      RETURN
      END
      SUBROUTINE GAUSS(A,B,N,M,IFLAG,LP,LQ,R)
C
C  SLOVES THE SYSTEM OF EQUATIONS NECESSARY FOR THE G.L.S.D.C.
C  ALGORITHM.
C
      IMPLICIT REAL*8 (A-H,O-Z)
      DOUBLE PRECISION A(N,N),B(N,M),LP(N),LQ(N,2),R(N)
      DO 5010 I=1,N
 5010    LP(I)=0
      DO 5150 K=1,N
         CON=0.
         DO 5050 L=1,N
            IF(LP(L).EQ.1) GO TO 5050
            DO 5040 J=1,N
               IF (LP(J)-1) 5030,5040,5200
 5030          IF(DABS(CON).GE.DABS(A(L,J))) GO TO 5040
               IR=L
               IC=J
               CON=A(L,J)
 5040       CONTINUE
 5050    CONTINUE
         LP(IC)=LP(IC)+1
         IF(IR.EQ.IC) GO TO 5090
         DO 5060 I=1,N
            CON=A(IR,I)
            A(IR,I)=A(IC,I)
 5060       A(IC,I)=CON
         IF (IFLAG.EQ.0) GO TO 5090
         DO 5070 I=1,M
            CON=B(IR,I)
            B(IR,I)=B(IC,I)
 5070       B(IC,I)=CON
 5090    LQ(K,1)=IR
         LQ(K,2)=IC
```

```
         R(K)=A(IC,IC)
         A(IC,IC)=1.
         DO 5100 I=1,N
 5100       A(IC,I)=A(IC,I)/R(K)
         IF(IFLAG.EQ.0) GO TO 5120
         DO 5110 I=1,M
 5110       B(IC,I)=B(IC,I)/R(K)
 5120    DO 5150 I=1,N
            IF(I.EQ.IC) GO TO 5150
            CON=A(I,IC)
            A(I,IC)=0.
            DO 5130 J=1,N
 5130          A(I,J)=A(I,J)-A(IC,J)*CON
            IF(IFLAG.EQ.0) GO TO 5150
            DO 5140 II=1,M
 5140          B(I,II)=B(I,II)-B(IC,II)*CON
 5150 CONTINUE
         DO 5170 I=1,N
            J=N-I+1
            IF(LQ(J,1).EQ.LQ(J,2)) GO TO 5170
            IR=LQ(J,1)
            IC=LQ(J,2)
            DO 5160 K=1,N
               CON=A(K,IR)
               A(K,IR)=A(K,IC)
               A(K,IC)=CON
 5160       CONTINUE
 5170 CONTINUE
 5200 RETURN
      END
      SUBROUTINE DUMP(TM,UM,NI,NJ)
C
C  EMPTIES THE CONTENTS OF MATRIX TM(NI,NJ) INTO UM(NI,NJ)
C
      IMPLICIT REAL*8(A-H,O-Z)
      DOUBLE PRECISION TM(NI,NJ),UM(NI,NJ)
      DO 6000 I=1,NI
         DO 6000 J=1,NJ
 6000       UM(I,J)=TM(I,J)
      RETURN
      END
```

The vita has been removed from the scanned document

ESTIMATION OF SPACECRAFT ATTITUDE IN THE PRESENCE OF UNMODELED DISTURBANCE TORQUES

by

Earl D. Pinson

(ABSTRACT)

A general approach is presented for the estimation of spacecraft attitude from rate gyroscope measurements of angular velocity and indirect inertial orientation measurements obtained from a pair of star sensors. The estimation algorithm is developed in such a way that the measured minus estimated angular velocity residuals are consistent with the apriori knowledge of the instrument error variance. The angular velocity history is modeled as a Fourier Series, whereas the attitude is modeled as the solution of the appropriate kinematic differential equations. The study presented addresses computer implementation issues and provides numerical results from several simulated attitude and velocity histories. The software is presented in FORTRAN code in an appendix.